

Supporting Information

Reversible Metal-Centered Reduction Empowers a Ni-Corrin to Mimic F430

Christopher Brenig,^a Dr. Leila Mosberger,^a Dr. Olivier Blacque,^a Dr. Reinhard Kissner^b and Prof. Dr. Felix Zelder^{a*}

^a*Department of Chemistry, University of Zurich, Winterthurerstrasse 190, CH-8057 Zurich, Switzerland. Fax: +41 44 635 6803; E-mail: felix.zelder@chem.uzh.ch, www.felix-zelder.net.*

^b*Institute of Inorganic Chemistry, ETH Zurich, Vladimir-Prelog-Weg 1-2, 8093 Zurich, Switzerland*

Contents

Materials and Methods.	S4
Reaction Schemes.	S8
- Scheme S1 Photo-oxygenolysis of DCCbs .	S8
- Scheme S2 Synthesis of 5,6-DONibs⁺ from 5,6-DODCCbs .	S8
- Scheme S3 Synthesis of Ni-1⁺ from 5,6-DONibs⁺ .	S9
Experimental Procedures.	S9
- Co_{αβ}-dicyano heptamethyl cobyrrinate (DCCbs).	S9
- 5,6-dioxo-5,6-<i>seco</i> Co_{αβ}- dicyano heptamethyl cobyrrinate (5,6-DODCCbs).	S9
- 5,6-dioxo-5,6-<i>seco</i>-heptamethyl nibyrrinate perchlorate (5,6-DONibs[ClO₄]).	S10
- (5<i>R</i>, 6<i>S</i>)-5,6-dihydroxy-5,6-dihydro heptamethyl nibyrrinate perchlorate (Ni-1[ClO₄]).	S11
Atom Numbering.	S12
- Figure S1 Atom numbering of Ni-1⁺ .	S12
Chromatograms and Optical spectra.	S13
- Figure S2 UV/Vis spectrum of 5,6-DONibs⁺ .	S13
- Figure S3 UV/Vis spectrum of Ni-1⁺ .	S13
- Figure S4 CD spectrum of Ni-1⁺ .	S14
- Figure S5 LC-chromatogram and ESI-MS spectrum of 5,6-DONibs⁺ .	S14
- Figure S6 LC-chromatogram and ESI-MS spectrum of Ni-1⁺ .	S14
NMR spectra, table of NMR data and discussion.	S15
- Figure S7 ¹ H-NMR spectrum of 5,6-DONibs⁺ .	S15
- Figure S8 ¹ H-NMR spectrum of Ni-1⁺ .	S15
- Figure S9 ¹ H- ¹ H-pQF-COSY spectrum of Ni-1⁺ .	S16
- Figure S10 ¹ H- ¹ H-ROESY spectrum of Ni-1⁺ .	S17
- Figure S11 ¹ H- ¹³ C-HSQC spectrum of Ni-1⁺ .	S18
- Figure S12 ¹ H- ¹³ C-HMBC spectrum of Ni-1⁺ .	S19
- Table S1 ¹ H-NMR chemical shifts and ¹³ C-NMR chemical shifts of Ni-1⁺ .	S19

EPR spectra.	S21
- Figure S13	S21
EPR spectrum of Ni-1⁺ in frozen MeCN at 110 K.	
- Figure S14	S21
Double integration of the deconvoluted broad signal of Ni-1⁺ .	
Electrochemical and Spectroelectrochemical data.	
- Figure S15	S22
Cyclic voltammograms of Ni-1⁺ in DMF.	
- Figure S16	S23
Cyclic voltammograms of Ni-1⁺ in CH ₃ CN.	
- Figure S17	S23
Cyclic voltammogram of Ni-1⁺ recorded in the SEC cell.	
- Figure S18	S24
UV/Vis spectroscopic changes upon reduction of Ni-1⁺ in the SEC cell.	
- Figure S19	S24
Absorption spectra of Ni-1⁺ and reduced Ni-1 recorded in the SEC cell.	
Computational.	S25
- Figure S20	S25
DFT optimized ground-state structure of Ni-1⁺ .	
- Table S2	S26
Coordinates of the DFT optimized ground-state structure of Ni-1⁺ .	
- Figure S21	S30
DFT optimized ground-state structure of Ni-1 .	
- Table S3	S30
Coordinates of the DFT optimized ground-state structure of Ni-1 .	
References.	S35

1 . Materials and Methods

General. Chemicals were of reagent grade quality or better, obtained from *Sigma–Aldrich*, *Merck* or *Fluka* and used without further purification. Vitamin B₁₂ was a generous gift from *DSM Nutritional Products AG* (Basel/Switzerland) and Prof. em. B. Jaun (ETH, Switzerland). All solvents were of reagent, analytical, gradient or LC-MS grade, respectively and obtained from commercial suppliers. Bidistilled H₂O was used in isolation and purification steps. H₂O from a Milli-Q (*Merck-Millipore*) water purification system was used for LC–MS measurements and when indicated. Reactions were carried out under N₂ (g) or Ar (g) in oven-dried (100 °C) glass equipment and monitored for completion by analysing a small sample (after suitable workup) by TLC or LC–MS. Extracts were washed with brine, followed by H₂O and dried over anhydrous Na₂SO₄ or passed through oven-dried cotton. Evaporation of the solvents *in vacuo* was done with the rotary evaporator at given bath temperature and pressure. Chromatography: silica gel 60 (40–63 µm, *Merck*) with the indicated solvent system. Thin layer chromatography (TLC): TLC plates (*Merck*); silica gel 60 on aluminium with the indicated solvent system; the spots were visualized by UV light (254 and 366 nm). Preparative TLC: *Merck* TLC glass plates (0.5 · 250 · 250 mm), silica gel, using the indicated solvent system. The bands containing the compound of interest were scraped from the TLC plate and the silica gel was subjected to extraction with 6.0 mL of CH₃OH containing 0.02 M NaClO₄ (2–3 min) in 15 mL glass centrifuge tubes. The suspension was subsequently centrifuged, and the liquid collected. The pellet was extracted again as mentioned above. The combined supernatants were diluted with H₂O (20 mL) and CH₃OH was removed *in vacuo*. Corrinoid material was isolated from the resulting aq. soln. using SPE. Preparative HPLC: *LaPrep* HPLC system (*VWR*) equipped with a PDA detector and a *Nucleodur 100-5* silica column (250 x 40 mm, *Machery–Nagel*). A gradient of CH₂Cl₂ (0 min 2% A, 0–40 min % A, 40–40.1 min 100% A, 40.1–50 min 100% A) of CH₃CN (solvent A) versus MeOH was applied using a flow rate of 60 mL min⁻¹. Solid Phase Extraction: *SepPak*® RP18 cartridges (*Waters*). Compounds were dissolved in MeCN/H₂O 1:9, transferred to the adsorbent, washed excessively with H₂O, and eluted with MeCN. UV/Vis spectra: *Cary Series* spectrophotometer (*Agilent technologies*) using 1 cm quartz cuvettes (*Hellma Analytics*); samples in CH₃OH, CHCl₃ or CH₃CN; λ_{max} (logε) in nm. CD spectroscopy: *JS 810* spectropolarimeter (*Jasco*) using 1cm quartz cuvettes at a scan rate of 100 nm min⁻¹. Temperature was maintained at 293 K with a *PFD-425S* temperature controller (*Jasco*); λ_{max}(θ), λ_{min}(θ) in nm (mdeg). IR spectra: *SpectrumTwo FT-IR Spectrometer* (*Perkin–Elmer*) equipped with a *Specac Golden Gate*TM ATR (attenuated total reflection)

accessory; applied as neat samples; $1/\lambda$ in cm^{-1} . NMR spectroscopy in CDCl_3 or CD_3OD at 500 MHz (^1H) or 128 MHz (^{13}C) and 298 or 278 K; *Avance III HD* 500 MHz spectrometer (*Bruker*) equipped with a *BOSS-II* shim system, a digital lock control unit, an *AMOS Control System*, a *DQD* unit, a *BVT3000* with a *BCU05* cooling unit and *GRASP Level II* for gradient spectroscopy, using a 5 mm BB inverse probehead (^1H , ^{13}C) with an actively shielded z-gradient coil and *ATM* or a *Cryo 5* mm QNP probe head (^{13}C) with an actively shielded z-gradient coil and *ATM*; δ in ppm rel. to CDCl_3 ($\delta^1\text{H}$ 7.26, $\delta^{13}\text{C}$ 77.06; corresponds to TMS (δ 0.00)) or CD_3OD ($\delta^1\text{H}$ 3.31, $\delta^{13}\text{C}$ 49.03; corresponds to TMS (δ 0.00)), J in Hz. LC-MS: *Acquity* UPLC system (*Waters*) equipped with a PDA detector and an autosampler using an *ACQUITY UPLC BEH C18 Gravity* 1.7 μm (2.1 mm \times 50 mm) reverse phase column (*Waters*). The UPLC system was connected to a *HCT* ESI-MS spectrometer (*Bruker Daltonics*). A total volume of 1 μL of an aq. sample soln. was analysed. A gradient (0 min 25% A, 0.1–4 min 100% A, 4.1–5 min 100% A) of CH_3CN (solvent A) versus an aq. soln. of 0.1% HCOOH (solvent B) was applied using a flow rate of 0.5 mL min^{-1} . All solvents used were of LC-MS grade. ESI-MS: *Bruker Daltonics HCT* with an ESI source operated in positive or negative mode. Injection rate 3 $\mu\text{L min}^{-1}$. Nebulizer P = 10 psi, dry gas flow rate 5 L min^{-1} , dry gas T = 350 $^\circ\text{C}$. All solvents used were of LCMS grade.

Electrochemistry: Cyclic voltammetry in analytical grade *N,N*-dimethylformamide (DMF) or MeCN (*Acros Organics*, kept over 3 \AA molecular sieve) using a *PGSTAT128N* potentiostat/function generator (*Metrohm Autolab*). Working electrode: 7.1 mm^2 glassy carbon disk; counter electrode: 2 mm glassy carbon rod (both *Metrohm Schweiz AG*). The working electrode was polished with 0.3 μm alumina powder/methanol paste and rinsed with methanol before each experiment. An Ag-wire was used as convenient pseudo reference electrode. It was experimentally confirmed during all voltammetry sessions that its potential difference to the ferrocenium/ferrocene (Fc^+/Fc) couple was stable within 5 mV for the chosen electrolyte. Potential scales were converted to SHE based on the known electrode potentials of Fc^+/Fc in organic solvents and in H_2O , measured against the aqueous Ag/AgCl, sat. KCl electrode.^{S1} Electrolyte soln. was prepared *in situ* by transferring Bu_4NPF_6 (1.93 g) into the dry voltammetry vessel, which then was assembled into the air-proof voltametric cell. Under N_2 (g) atmosphere (99.99%, dry), DMF (5.0 mL) was added by means of a gas-tight glass syringe. The resulting 0.1 M electrolyte soln. was de-aerated with N_2 for 15 mins. A blank scan was taken at each scan rate to be examined, before 200 μL of a soln. of **Ni-1**[ClO_4] (5.0 mg) in DMF (0.5 mL) were added. The solution was de-aerated again for 15 mins, before three cyclic

scans in the indicated potential range were taken at a scan rate of 0.1 Vs^{-1} . Electrocatalytic generation of acetonitrile from 1-chloroacetonitrile (CAN) was probed with cyclic voltammetry using the following conditions: **Ni-1**[ClO₄] (2.5 mg, 0.42 mM) in DMF (5.0 mL) containing 0.1 M Bu₄NPF₆, working electrode: 2 mm glassy carbon rod; Counter electrode: Pt-disc; Quasi-reference electrode: Ag-wire, reference: Fc/Fc⁺ couple, 0.1 V/ min; Start potential: -0.3 V ; Lower vertex potential: -1.3 V ; Upper vertex potential: 0 V ; Titrations with increasing amounts of CAN were conducted by addition of the respective amount of CAN into the bulk soln., followed by de-aeration with N₂ (15 mins.) and thorough mixing of the soln. using the counter electrode's rotation. All potentials given vs. SHE. DMF (99.9%, extra dry) was from ACROS Organics, Bu₄NPF₆ and CAN (99.8%) were from Sigma–Aldrich.

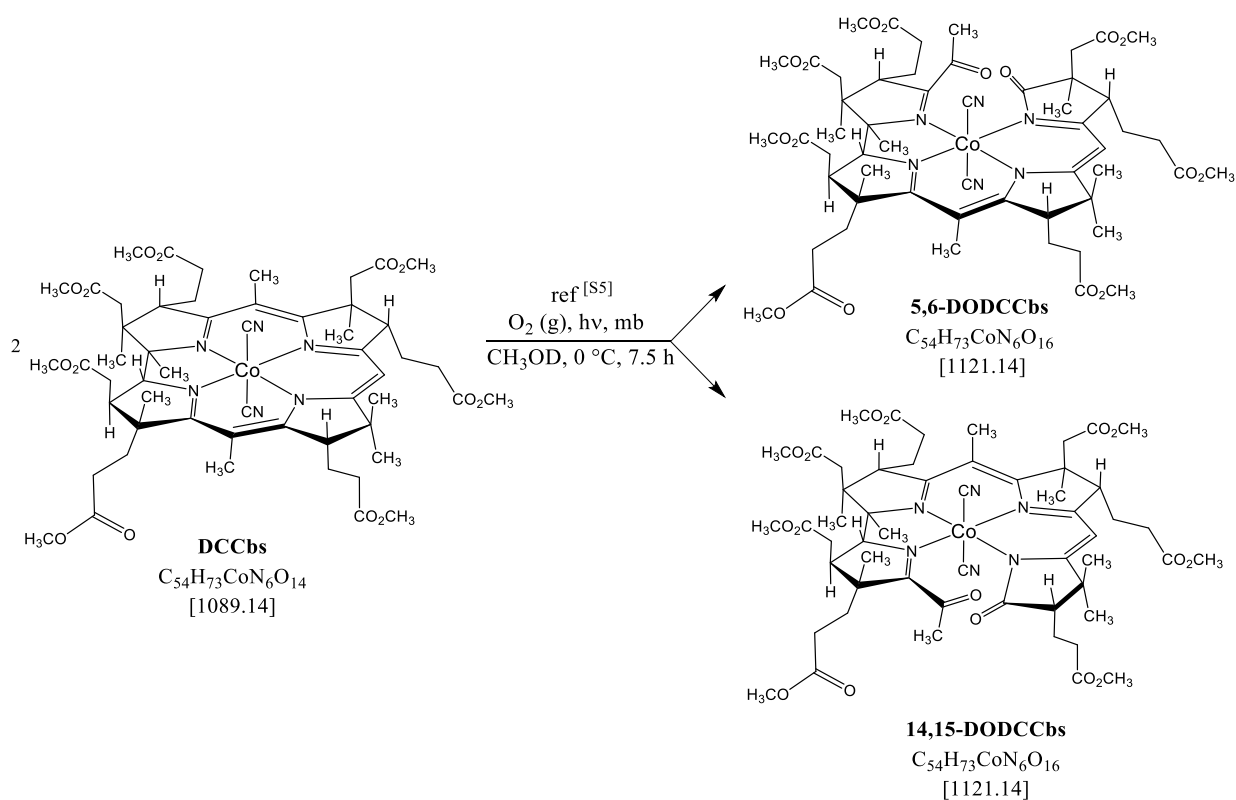
Spectroelectrochemistry: A soln. of **Ni-1**[ClO₄] (1.5 mg, 2.56 mM) in MeCN (0.5 mL, containing 0.6 M Bu₄NPF₆) was transferred into an optically transparent thin layer electrochemical cell (SEC) with a Pt-mesh working and counter electrode and a Ag quasi-reference electrode.^{S2} The cell was equipped with CaF₂ windows. UV/Vis/NIR spectra (150–900 nm) were recorded using an *USB4000* optical fiber diode array spectrometer (*Ocean Optics*) with a *DH-2000-BAL* UV/Vis–NIR light source (*Mikropak*), applying an integration time of 10 ms. Cyclic voltammetry scans were performed with a *Vertex* potentiostat (*Ivium*) applying a start potential of 0 V vs. Ag-quasi-reference and a return potential of -1.5 V vs. Ag-quasi-reference at a scan rate of 10 mV/s . A trigger scheme was used to synchronize the electrochemical data acquisition (*IviumSoft*) and the spectroscopic measurements (*OO SpectraSuite*) using a four-channel digital delay/ pulse generator (*Stanford Research Systems, Inc.*). This measurement setup also enabled protection of the sample from irradiation by closing the shutter of the light source when no data was acquired. Additionally, platinum sputtered CaF₂ windows were used as neutral density filters to attenuate the light coming from the source via an optical fiber fitted with a collimating lens. The applied potential was calibrated externally using the Fc⁺/Fc redox couple in Bu₄NPF₆ soln. (0.6 M) in MeCN (0.5 mL). All potentials given in V vs. SHE.

EPR Experiments. Sample Preparation: Reductions were carried out in MeCN containing 0.1 M Bu₄NBF₄ or Bu₄NPF₆ electrolytes, in a two-compartment electrolysis cell under nitrogen atmosphere. Compartments were separated by a polypropylene membrane grafted with anion exchanging quaternary ammonium groups. The cathode compartment contained **Ni-1**[ClO₄] (5.0 mg) dissolved in electrolyte solution, a platinum sheet as working electrode and a silver wire as a pseudo-reference electrode. The anode compartment contained a coiled silver wire as

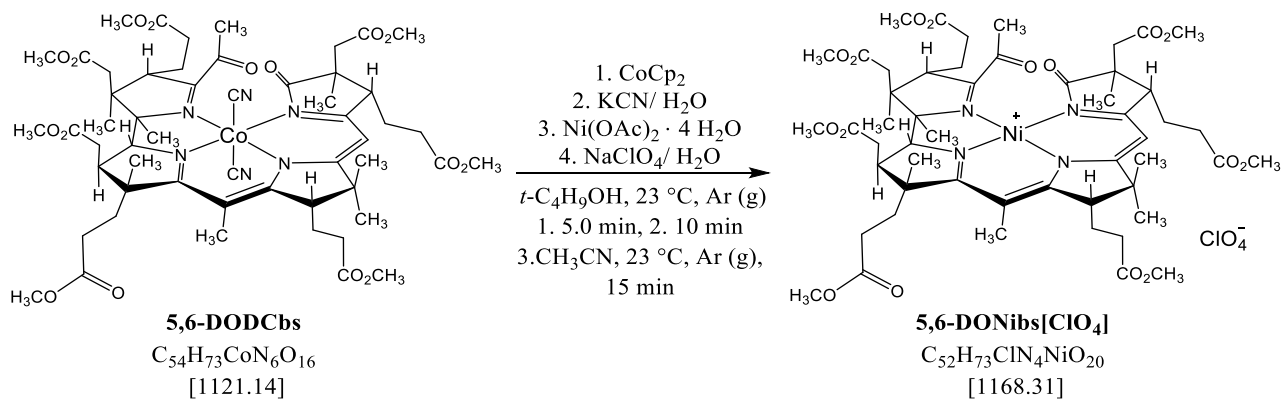
counter electrode and electrolyte solution. Prior to electrolysis, a cyclic voltammetry scan was performed to identify the peak potential of the first reduction wave of **Ni-1⁺**/ **Ni-1**. For electrolysis, the working potential was set slightly more negative (ca. 50 mV) than this peak potential, in order to avoid over-reduction which had been observed in cyclic voltammetry studies. During potentiostatic electrolysis, the current was monitored. The initial current dropped and asymptotically approached a limiting value after 10–15 minutes, which was interpreted as completion of the desired reduction. Reduction was accompanied by color change of the cathode compartment solution. MeCN of the reduced solution was partially evaporated by passing through a N₂ (g) in order to concentrate the sample. The solution was then collected with a gas tight syringe conditioned with N₂ (g) and brought into a glove box where it was transferred into a quartz EPR tube. The latter was sealed and taken out of the glove box. The sample was immediately frozen in N₂ (l) and kept there until it was mounted in the spectrometer. *EPR measurements*: The Dewar tube in the cavity of the 5000 CW X-band EPR spectrometer (*Magnettech*) was pre-cooled to 110 K. The sample was inserted, centered and conditioned to 110 K. Because of the low sample concentration, 21 to 30 scans were accumulated and averaged.

DFT Calculations. Density functional theory (DFT) calculations were carried out using the *Gaussian 09* program package.^{S3} The hybrid functional B3LYP^{S4} was chosen in association with the standard 6-31+G(d) basis set^{S5} and the conductive polarizable continuum model (CPCM)^{S6,S7} for the solvent effects (CH₃CN). The optimized geometries of **Ni-1⁺** and **Ni-1** were confirmed to be potential energy minima by vibrational frequency calculations at the same level of theory (for cartesian coordinates see Tables S2 and S3).

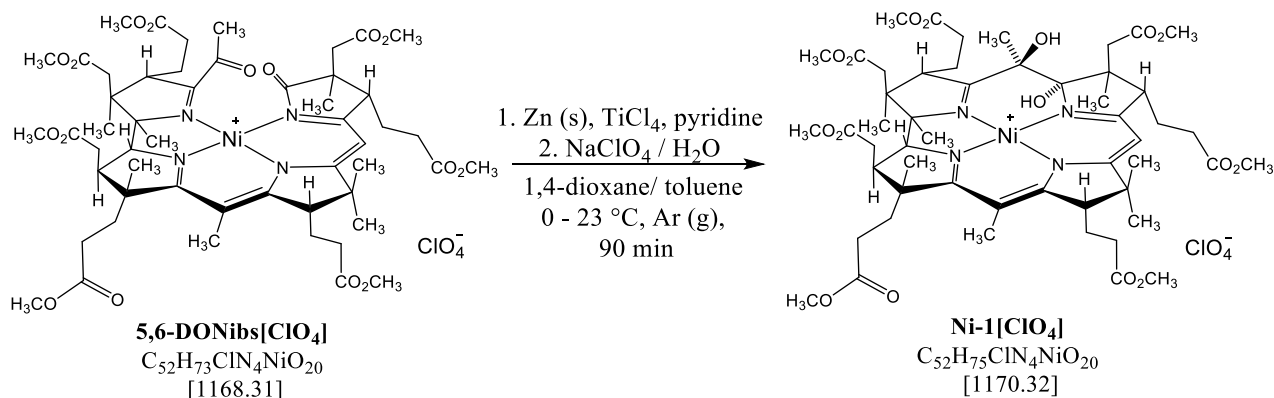
Reaction Schemes.



Scheme S1. Photo-oxygenolysis of DCCbs.



Scheme S2. Synthesis of 5,6-DONibs⁺ from 5,6-DODCCbs.



Scheme S3. Synthesis of Ni-1⁺ from 5,6-DONibs⁺.

Experimental Procedures.

Co_{αβ}-dicyano heptamethyl cobyrinate (DCCbs).

DCCbs was synthesized using known literature procedures with the modifications introduced by Marques *et al.*,^{S8} based on the original procedure by Werthemann.^{S9} in 87 % yield. After column chromatography (50 g SiO₂, 316 mg KCN, CH₂Cl₂/CH₃OH 10:0.1 – 10:0.3, gradually in 0.5 % steps), DCCbs was obtained in 87% yield. *Co_{αβ}-dicyano heptamethyl cobyrinate*: TLC: *R_f* = 0.74 (EtOAc/CH₃OH 9:1). UV/Vis (CH₃OH, *c* = 5.4 · 10⁻⁵m): 280 (3.90), 313 (3.83), 369 (4.33), 420 (3.24), 510 (*sh.*, 3.45), 545 (3.78), 585 (3.86). IR: 3446_w, 2953_w (C–H), 2123_w (C≡N), 1727_s (C=O), 1580_m, 1501_s, 1435_m, 1402_m, 1367_m, 1353_m, 1300_m, 1198_s (C–O), 1150_s, 1104_s, 1003_m, 884_w, 858_w, 804_w. ¹H-NMR (CD₃OD, *c* = 5.4 · 10⁻³ M): 5.81 (*s*, HC10), 3.86 (*d*, *J* = 10.5, HC19), 3.84–3.82 (*m*, HC3), 3.81 (*s*, H₃CO₂C182), 3.76 (*s*, H₃CO₂C22), 3.75 (*s*, H₃CO₂C72), 3.73 (2 *s*, H₃CO₂C33, H₃CO₂C173), 3.71 (*s*, H₃CO₂C83), 3.65 (*s*, H₃CO₂C133), 3.47 (*dd*, *J* = 8.0, 4.9, HC8), 3.24 (*dd*, *J* = 6.0, 4.4, HC13), 2.90 (*dd*, *J* = 10.6, 3.6, HC18), 2.85–2.75 (*m*, *H_a* of H₂C71, H₂C181), 2.74–2.57 (*m*, *H_a* of H₂C21, H₂C172, H₂C32), 2.57–2.38 (*m*, *H_b* of H₂C71, H₂C21, *H_a* of H₂C171, H₂C82), 2.34 (*s*, H₃C151), 2.32–2.21 (*m*, *H_b* of H₂C172, H₂C132, *H_a* of H₂C81, H₂C131, H₂C31) superimposed by 2.29 (*s*, H₃C51), 1.91–1.82 (*m*, *H_b* of H₂C131, H₂C171), 1.74 (*dt*, *J* = 8.5, 4.5, *H_b* of H₂C81), 1.66 (*s*, H₃C7A), 1.53 (*s*, H₃C1A), 1.46–1.45 (2 *s*, H₃C2A, H₃C12A), 1.32 (*s*, H₃C17B); 1.32 (*s*, H₃C12B) LC–MS (MS⁺): *R_t* = 2.40 min, *m/z* = 1062.53 (100, [M–CN]⁺, *m/z*_{calc}: 1062.45 for C₅₃H₇₃CoN₅O₁₄⁺).

5,6-dioxo-5,6-*seco* Co_{αβ}- dicyano heptamethyl cobyrinate (5,6-DODCCbs).

Photo-oxidation of DCCbs was performed based on a procedure developed by Krätler and Stepánek.^{S10} DCCbs (179 mg, 164 μmol) and methylene blue (1.90 mg, 5.94 μmol, 3.8 mol-%) were dissolved in CH₃OD (10 mL) and transferred into a photoreactor. The water-cooled soln. was purged with O₂ prior to irradiation. The oxygen saturated mixture was irradiated with a 240 W halogen lamp for 7.5 h. The solvent was evaporated *in vacuo* (300 mbar, 40 °C).

Desired **5,6-DODCCbs** was separated from its region-isomeric counterpart 14,15-dioxo Co $\alpha\beta$ -dicyano heptamethyl cobyrinate (**14,15-DODCCbs**) as well as some unreacted starting material by preparative HPLC. Pure fractions were pooled, and the solvent was evaporated *in vacuo* (650 mbar, 40 °C). The residues of **5,6-DODCCbs** and **14,15-DODCCbs** were dissolved in EtOAc (0.2 mL), respectively, and *n*-hexane (3.0 mL) was added. The resulting precipitates were vortexed and centrifuged (3500 rpm, 15 min). The solvent was decanted and both solids were dried under high vacuum yielding **5,6-DODCCbs** (75.0 mg, 66.9 μ mol, 41 %) as a red solid and **14,15-DODCCbs** (60.7 mg, 54.1 μ mol, 33%) as a red-brown solid. *5,6-dioxo-5,6-seco Co $\alpha\beta$ -dicyano heptamethyl cobyrinate*: UV/Vis (CHCl₃, $c = 4.5 \cdot 10^{-5}$ M): 276 (*sh.*, 3.99), 392 (*sh.*, 3.90), 330 (3.96), 367 (*sh.*, 3.45), 490 (*br.*, 3.92). IR: 3446_w, 2954_w (C–H), 2163_w, 2126_w (C \equiv N), 1725_s (C=O), 1634_w, 1556_w, 1531_w, 1498_m, 1436_m, 1402_m, 1372_m, 1307_m, 1172_s, 1100_s, 1048_m, 1006_s, 887_w, 849_w, 819_w. ¹H-NMR (CDCl₃, $c = 4.5 \cdot 10^{-3}$ M): 5.55 (*s*, HC10), 3.81–3.65 (*m*, HC19, HC3) superimposed by 3.78 (*s*, H₃CO₂C), 3.74 (*s*, H₃CO₂C), 3.72 (*s*, H₃CO₂C), 3.69 (2 *s*, 2 H₃CO₂C) and 3.67 (*s*, H₃CO₂C), 3.58 (*s*, H₃CO₂C), 3.27 (*dd*, $J = 8.6, 3.2, 1$ H, corrin-CH), 3.00 (*app. d*, $J = 4.2, 1$ H, corrin-CH), 2.91 (*t*, $J = 4.9$, corrin-CH), 2.77–2.28 (*m*, 12 corrin-CH and corrin-CH₂) superimposed by 2.66 (*s*, H₃C51), 2.25–2.18 (*m*, 7 corrin-CH and corrin-CH₂) superimposed by 2.21 (*s*, H₃C151) and 1.99 (*s*, corrin-CH₃), 1.76–1.63 (*m*, 4 corrin-CH₂), 1.30 (*s*, corrin-CH₃), 1.26 (*s*, corrin-CH₃), 1.24 (*s*, corrin-CH₃), 1.20 (*s*, corrin-CH₃), 1.00 (*s*, corrin-CH₃) LC–MS (MS⁺) : R_t = 2.20 min, $m/z = 1094.52$ (100, [M – CN]⁺, m/z_{calc} : 1094.44 for C₅₃H₇₃CoN₅O₁₆⁺).

5,6-dioxo-5,6-seco-heptamethyl nibyrinate perchlorate (5,6-DONibs[ClO₄]).

In a *Schlenk* tube, **5,6-DODCCbs** (32.0 mg, 28.5 μ mol) was dissolved in ^tBuOH (5.0 mL) at 23 °C. The soln. was degassed thoroughly by freeze-pump-thaw cycling (3 cycles) before CoCp₂ (10.8 mg, 57.1 μ mol, 2.0 equiv.) was added under Ar (g) counterflow. The soln. turned dark immediately and was stirred under Ar (g) at 23 °C for 5.0 min, before KCN (250 mg, 3.84 mmol, 135 equiv.) was added to the mixture followed by H₂O (2.0 mL), upon which the soln. turned bright yellow. After stirring at 23 °C for further 10 min, reaction control by LC–MS showed complete consumption of the starting material. The mixture was filtered through *Celite*® plug and the solid residue was washed with a few mL of ^tBuOH/H₂O (20 mL). The filtrates were combined and ^tBuOH was evaporated *in vacuo* (30 mbar, 20 °C). NaClO₄ (2M in H₂O) was added to the aq. phase which then was extracted with CH₂Cl₂ (3 \times 20 mL). The combined organic phases were filtered through cotton and the solvent was evaporated *in vacuo* (300 mbar, 21 °C) to approx. 1/10 of its original volume. The residual solvent was removed in a stream of Ar (g) until a yellow solid was observed. Metal-free 5,6-dioxo heptamethyl hydrogenobyrinate (**X**) was used without further purification in the re-metallation step. The yellow residue was dissolved in MeCN (anhydr., 5.0 mL) and the soln. was degassed by purging with Ar (g) for 15 min, before Ni(OAc)₂ \cdot 4 H₂O (72.1mg, 290.0 μ mol, 10 equiv.) was added. The yellow soln. turned orange immediately and was stirred under Ar (g) until reaction control by UPLC-MS showed full conversion of starting material (15 min). Then, H₂O (10 mL) and NaClO₄ (2M in H₂O, 5.0 mL) was added. CH₃CN was evaporated *in vacuo* (50 mbar, 20 °C) and the remaining aq. phase was extracted with CH₂Cl₂ (3 \times 15 mL). The solvent of the combined organic phases was evaporated *in vacuo* (450 mbar, 21 °C). The remaining solid was

dissolved in CH₃CN (1.5 mL) and lyophilized overnight to yield the perchlorate salt **5,6-DONibs[ClO₄]** (36.0 mg, 30.0 μmol, *quant.*) as an orange solid. *5,6-dioxo-5,6-seco-heptamethyl nibyrinate perchlorate*: UV/Vis (CH₃CN, $c = 2.5 \cdot 10^{-5}$ M): 259 (3.88), 276 (3.93), 318 (*sh.*, 3.71), 358 (*sh.*, 3.54), 459 (3.79). ¹H-NMR (CDCl₃, $c = 4.6 \cdot 10^{-3}$ M): 5.74 (*s*, HC10), 3.93 (*d*, $J = 11.0$, HC19), 3.75 (*s*, OCH₃), 3.73 (*s*, OCH₃), 3.73–3.65 (*m*, corrin-CH) superimposed by 3.70, 3.71 (2 *s*, 2 OCH₃), 3.68 (*s*, OCH₃), 3.66 (*s*, OCH₃) and 3.64 (*s*, OCH₃), 3.04–3.01 (*m*, corrin-CH), 2.99 (*s*, H₃C51), 2.95 (*t*, $J = 5.1$, corrin-CH), 2.89–2.84 (*m*, corrin-CH), 2.77–2.70 (*m*, 2 corrin-CH), 2.62 (*d*, $J = 14.7$, corrin-CH), 2.59–2.45 (*m*, corrin-CH, 2 corrin-CH₂), 2.44–2.39 (*m*, corrin-CH₂), 2.20 (*s*, H₃C151), 2.11 (*s*, corrin-CH₃), 2.09–2.03 (*m*, corrin-CH₂), 2.00–1.85 (*m*, 3 corrin-CH₂), 1.75–1.66 (*m*, 2 corrin-CH₂), 1.39 (*s*, corrin-CH₃), 1.32, 1.31 (2 superimposed *s*, 2 corrin-CH₃), 1.19 (*s*, corrin-CH₃), 0.97 (*s*, corrin-CH₃). LC-MS (MS⁺): $R_t = 2.49$ min, $m/z = 1067.54$ (100, M^+ , m/z_{calc} : 1067.44 for C₅₂H₇₃N₄NiO₁₆⁺).

(5*R*, 6*S*)-5,6-dihydroxy-5,6-dihydro heptamethyl nibyrinate perchlorate (Ni-1[ClO₄]).

In a *Schlenk* tube, Zn dust (60.0 mg, 0.91 mmol, 30 equiv.), previously dried in high vacuum (100 °C) was suspended in dioxane (anhydr., 2.0 mL). The suspension was cooled to 0 °C in an ice–water bath, before TiCl₄ (1.0 M in toluene, 0.48 mL, 0.48 mmol, 16 equiv.) was added under Ar (g) at 0 °C. To the resulting yellow mixture, pyridine (15.0 μL, 0.19 mmol, 6.0 equiv.) was added, resulting in a colour change to dark brown. The resulting mixture was refluxed (110 °C) for 1 h before it was cooled down to 23 °C. To the resultant black slurry, **5,6-DONibs[ClO₄]** (36.8 mg, 0.03 mmol, 1.0 equiv.) was added as a soln. in dioxane (anhydr., 1.0 mL) under Ar (g) over the course of 1h. The soln. turned brighter gradually and was stirred for another 30 min, before reaction control via LC–MS confirmed full conversion of the starting material. A saturated soln. of NaHCO₃ (10 mL) was added and the resulting pale grey slurry was filtered through *Celite*[®]. The residue and the aq. phase were thoroughly extracted with CH₂Cl₂ (3 x 15 mL), the combined org. phase was dried by filtration through cotton, and the solvent was removed *in vacuo* (380 mbar, 20 °C). The residue was purified with prep. TLC (5 % MeOH ([NaClO₄] = 0.02 M) vs. CH₂Cl₂) resulting in separation of a major yellow band, containing the desired ring-closed product **Ni-1⁺**. The band was isolated, and after evaporation of the solvents *in vacuo* (50 mbar, 20 °C), the remaining aq. soln. was extracted using SPE. The absorbed product was washed with H₂O ([NaClO₄] = 0.2 M, 10 mL), followed by H₂O (10 mL) and eluted with CH₃CN (2.5 mL). The soln. was lyophilized overnight to obtain **Ni-1[ClO₄]** (12.0 mg, 0.01 mmol, 33 %). *(5R, 6S)-5,6-dihydroxy-5,6-dihydro heptamethyl nibyrinate perchlorate*: UV/Vis (CH₃CN, $c = 7.6 \cdot 10^{-5}$ M): 263 (3.86), 277 (3.87), 316 (*sh.*, 3.52), 366 (*sh.*, 3.36), 447 (3.75). CD (CH₃CN, $c = 3.8 \cdot 10^{-4}$ M): λ_{min} 222 (–10.8), λ_{min} 249 (–5.9), λ_{min} 279 (–6.8), λ_{max} 318 (7.8), λ_{max} 370 (1.9), λ_{min} 433 (–21.9), λ_{max} 509 (10.2). ¹H-NMR (CDCl₃, $c = 2.3 \cdot 10^{-3}$ M): 5.57 (*s*, HC10), 3.76–3.65 (*m*, HC19) superimposed by 3.74 (*s*, OCH₃), 3.73 (*s*, OCH₃), 3.70 (2 *s*, 2 OCH₃), 3.68 (2 *s*, 2 OCH₃) and 3.66 (*s*, 2 OCH₃), 3.21 (*d*, $J = 16.7$, HC3, HC8), 2.98–2.65 (*m*, HC13, HC18, H₂C181), 2.49, 2.48 (2 *s*, HOC5, HOC6), 2.59–2.55 (*m*, H_a of H₂C21 and H₂C131), 2.22–2.17 (*m*, H_b of H₂C21) superimposed by 2.20 (*s*, H₃C151), 2.11–2.05 (*m*, H_a of H₂C31 and H₂C7), 1.75–1.71 (*m*, H_b of H₂C131), 1.67–1.60 (*m*, H_b of H₂C31, H_a of H₂C81) superimposed by 1.63 (*s*, H₃C51), 1.56 (*s*, H₃C1A), 1.45–1.40 (*m*, H_b of H₂C81, H_a of H₂C172), 1.39–1.36 (*m*, H₂C32), 1.35–1.30 (*m*, H_b of H₂C71, H_a of H₂C171) superimposed by 1.32 (*s*, H₃C7A), 1.30–1.20 (*m*, H_b of H₂C171, H₂C132)

superimposed by 1.24 (H_3C12A), 1.18–1.16 (m , H_a of H_2C172), 1.03–0.99 (m , H_2C82) superimposed by 1.01 (s , H_3C2A), 0.94 (s , H_3C12B). ^{13}C -NMR ($CDCl_3$): 181.0 (C11), 173.8 (C83), 173.0 (C22), 172.6 (C133, C33), 172.3 (C72, C173), 171.9 (C16), 171.0 (C182), 159.8 (C14), 158.6 (C4), 121.4 (C6), 107.5 (C15), 92.8 (C10), 76.0 (C5), 70.6 (C19), 58.5 (C3), 55.2 (C8, C18), 52.3 (OC25, OC36, OC86, OC75, OC136, OC176, OC185), 49.9 (C1), 49.5 (C12), 47.9 (C2, C7), 44.9 (C2), 40.2 (C181), 34.7 (C172), 34.5 (C17), 34.3 (C172), 31.2 (C131), 30.8 (C21), 30.7 (C13, C71), 30.1 (C82), 29.8 (C12A), 28.9 (C171), 27.9 (C32), 24.7 (C31), 23.8 (C51), 21.8 (C1A), 20.5 (C7A, C12B), 19.6 (C81), 18.0 (C17B), 15.2 (C151), 13.8 (C2A). LC-MS (MS^+): $R_t = 2.65$ min, $m/z = 1069.61$ (100, M^+ , m/z_{calc} : 1069.45 for $C_{52}H_{75}N_4NiO_{16}^+$).

Atom Numbering.

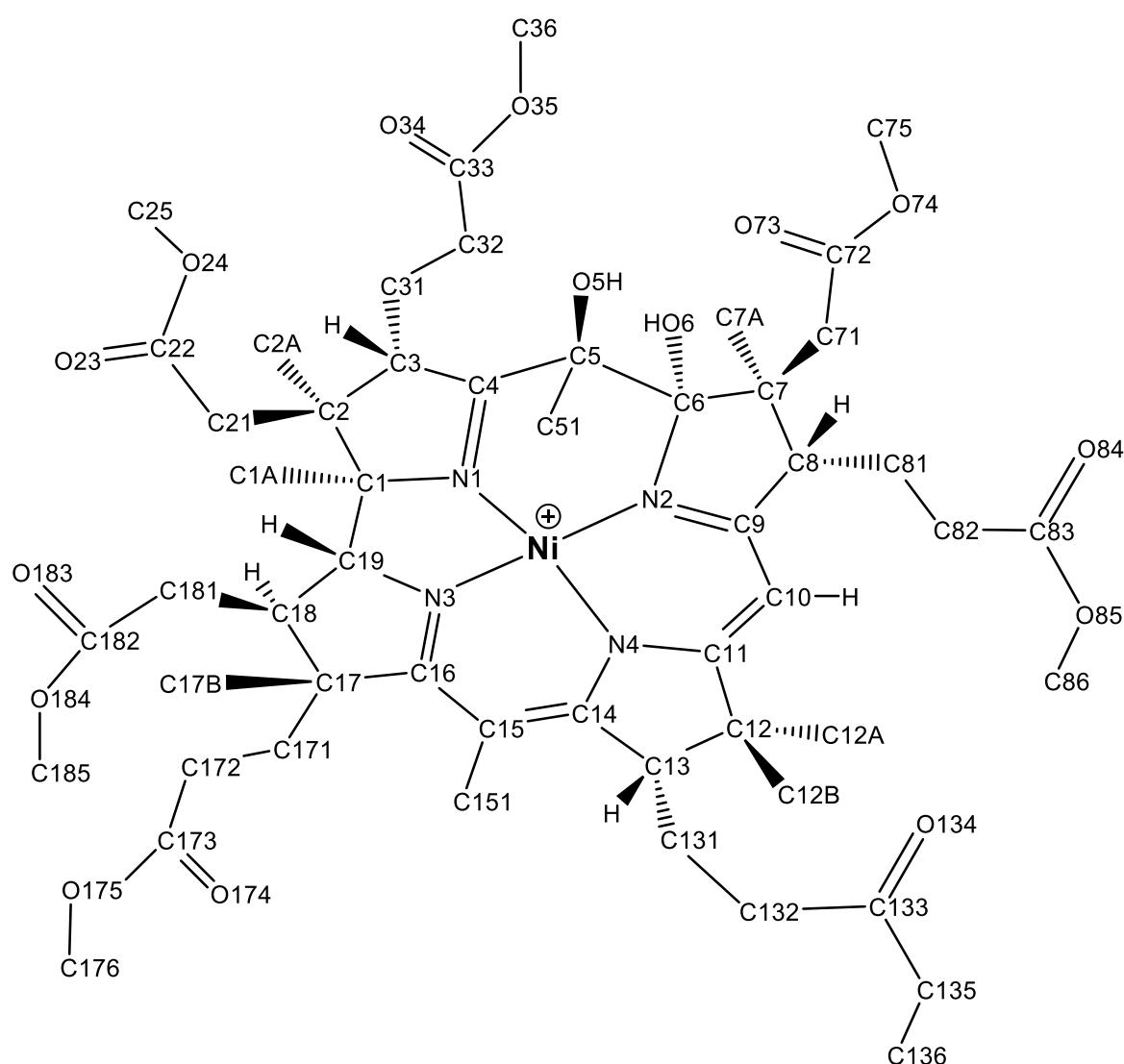


Figure S1. Atom numbering of Ni-1⁺.

Chromatograms and Optical spectra.

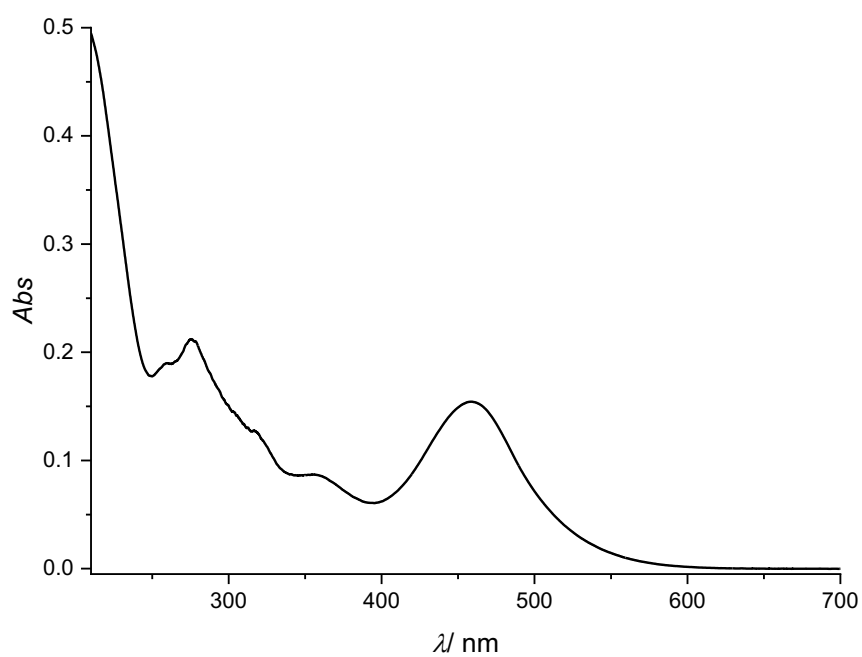


Figure S2. UV/Vis spectrum of **5,6-DONibs⁺** (CH_3CN , $c = 2.5 \cdot 10^{-5} \text{ M}$).

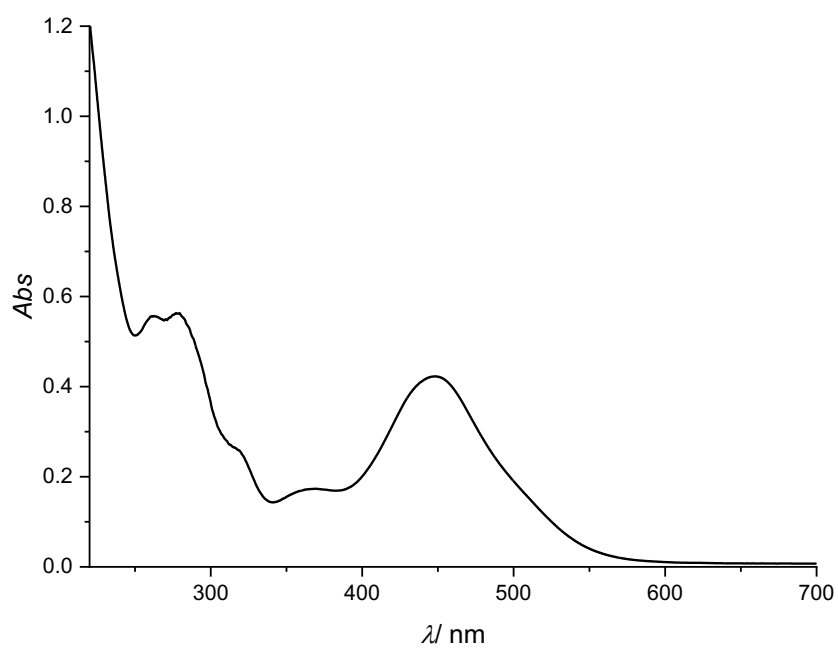


Figure S3. UV/Vis spectrum of **Ni-1⁺** (CH_3CN , $c = 2.5 \cdot 10^{-5} \text{ M}$).

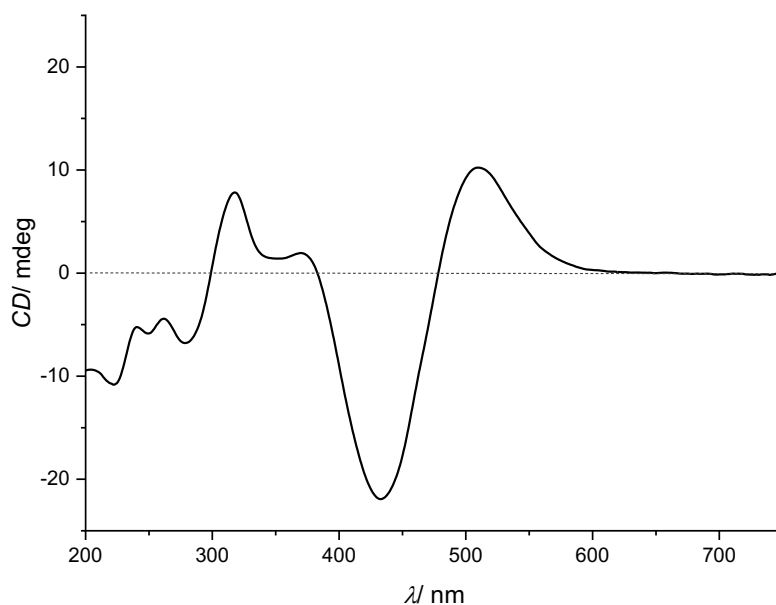


Figure S4. CD spectrum of **Ni-1⁺** (CH_3CN , $c = 3.8 \cdot 10^{-4} \text{ M}$).

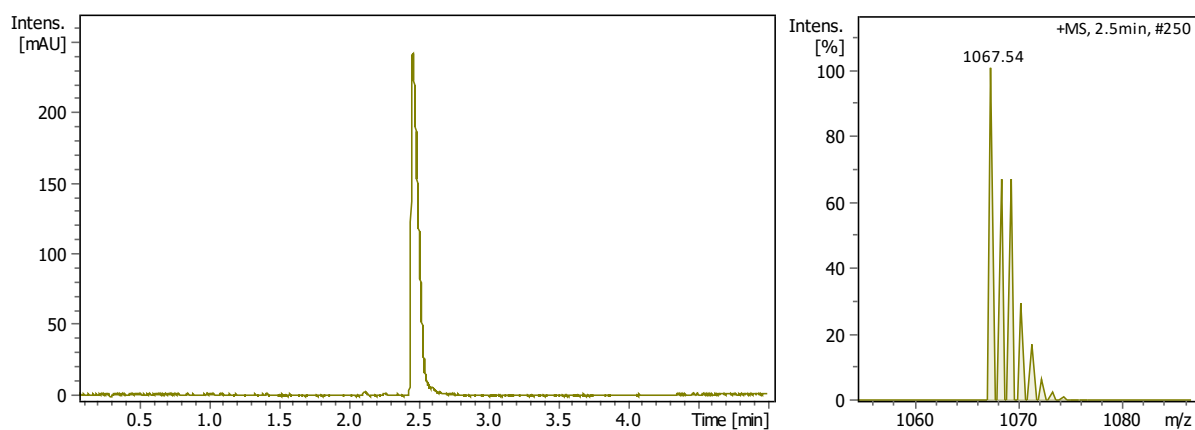


Figure S5. UHPL chromatogram of **5,6-DONibs⁺** (H_2O ($[\text{HCOOH}] = 0.1\%$)/ MeCN , 200–480 nm). *Right:* Section of the ESI-MS spectrum of **5,6-DONibs⁺**.

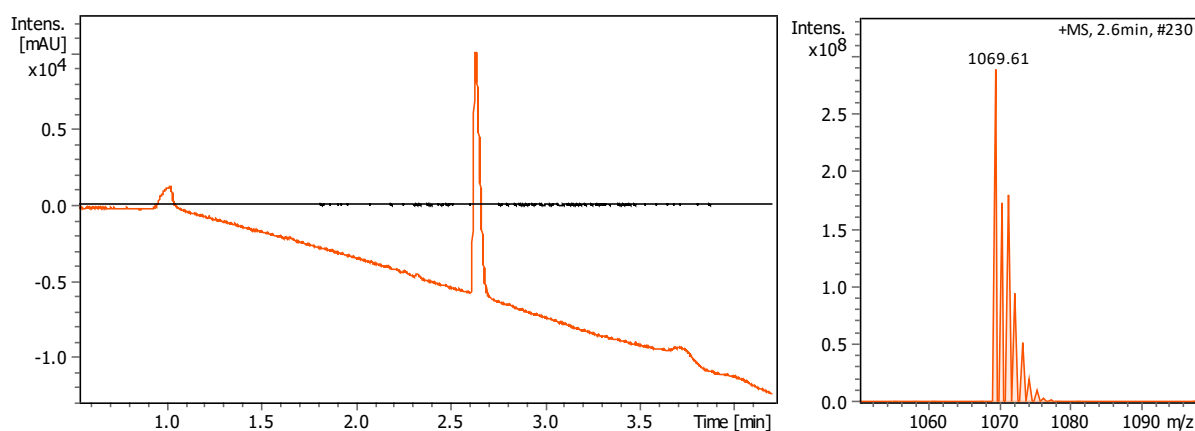


Figure S6. UHPL chromatogram of **Ni-1⁺** (H_2O ($[\text{HCOOH}] = 0.1\%$)/ MeCN , 200–480 nm). *Right:* Section of the ESI-MS spectrum of **Ni-1⁺**.

NMR spectra, table of NMR data and discussion.

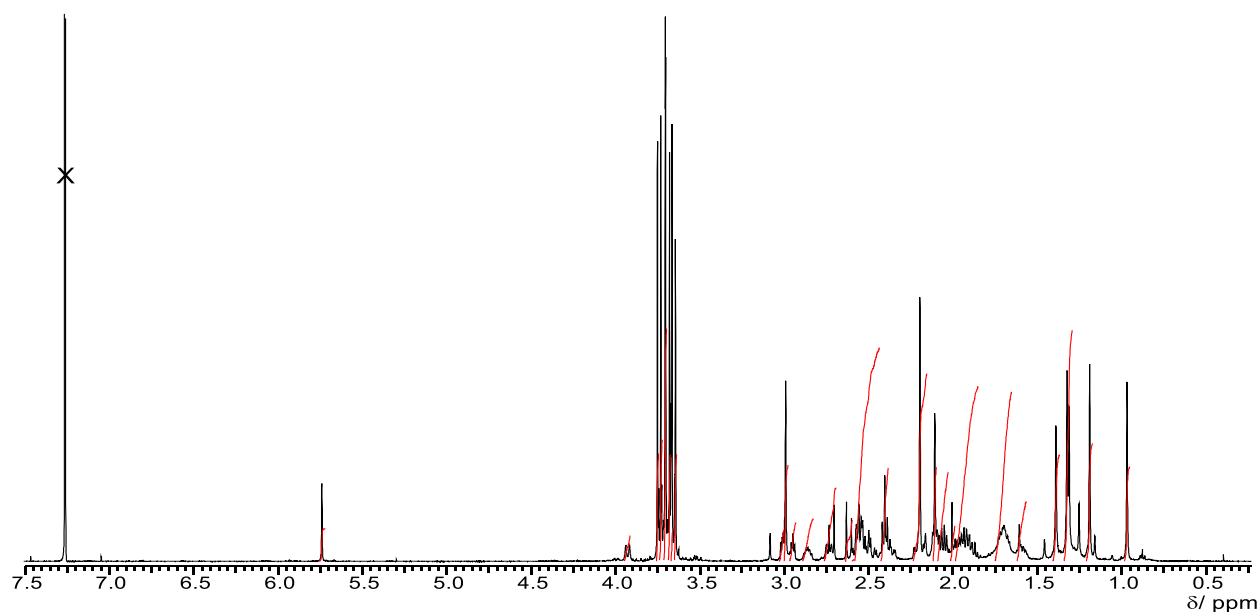


Figure S7. ¹H-NMR spectrum of **5,6-DONibs⁺** (500 MHz, CDCl₃, 298 K, 4.6 · 10⁻³ M).

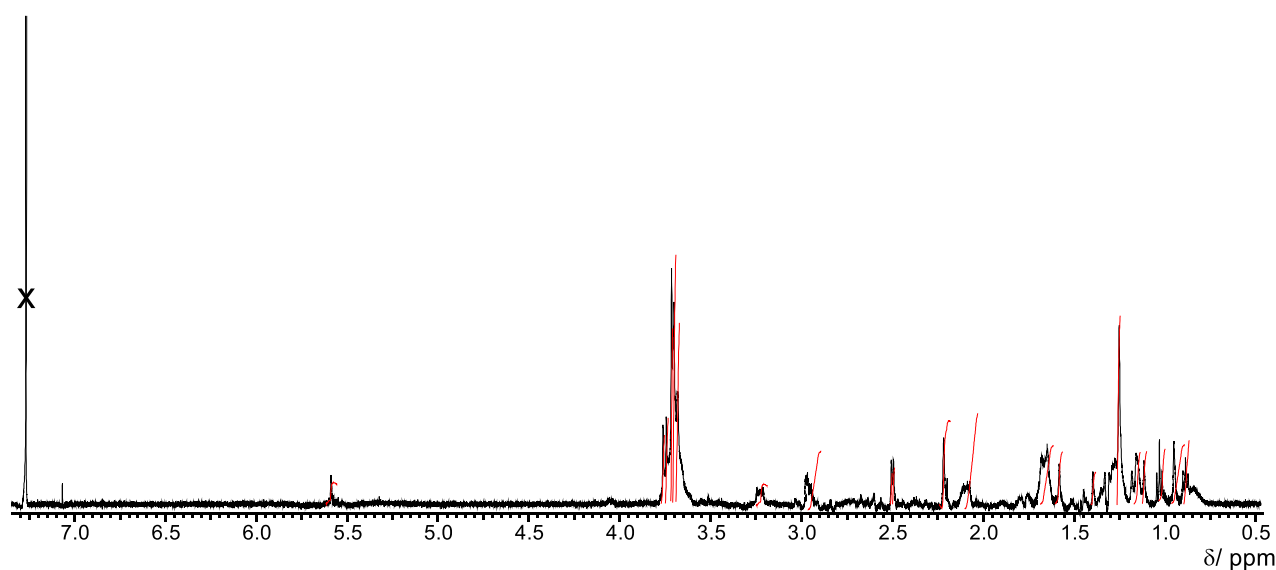


Figure S8. ¹H-NMR spectrum of **Ni-1⁺** (500 MHz, CDCl₃, 298 K, 2.2 · 10⁻³ M).

Comment: Highfield shifts ($\Delta\delta$ 0.3–1.3 ppm) were detected for the proton at C19 (3.36 ppm) as well as for the C51 methyl group (1.63 ppm), located in vicinity of the newly formed *trans*-diol unit in **Ni-1⁺**, when compared to the ¹H-NMR signals found for **5,6-DONibs⁺**. The signals of the two adjacent hydroxy groups were located at 2.46 and 2.47 ppm and, thus, display typical shifts for tertiary alcohol groups. ¹H-¹³C-HMBC spectroscopy, a particularly useful tool applied earlier for the structural determination of related 5,6-dihydroxy-nibalamine,^{S11} allowed for univocal establishment of the newly formed bond between C5 and C6 in **Ni-1⁺** via correlations between the C51 methyl group protons and the beforementioned carbons, located at 76.0 and 121.4 ppm, respectively.

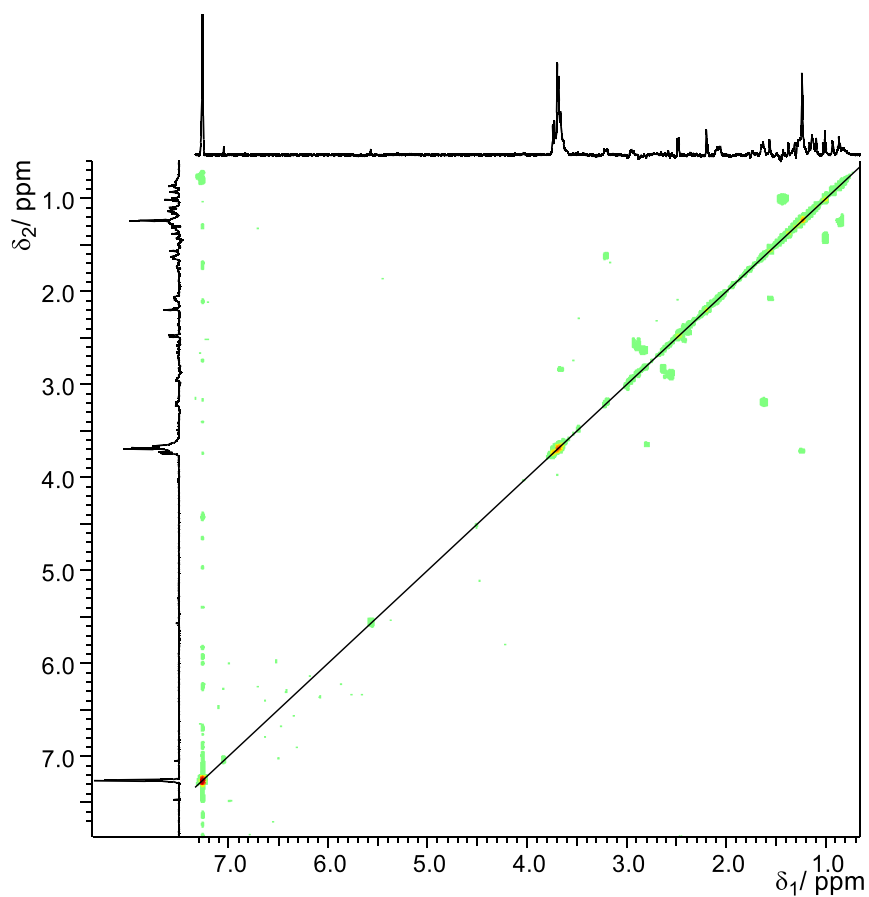


Figure S9. ^1H - ^1H -pQF-COSY spectrum of Ni-1^+ (500 MHz, CDCl_3 , 278 K, 4096 x 1024 p, 16 scans).

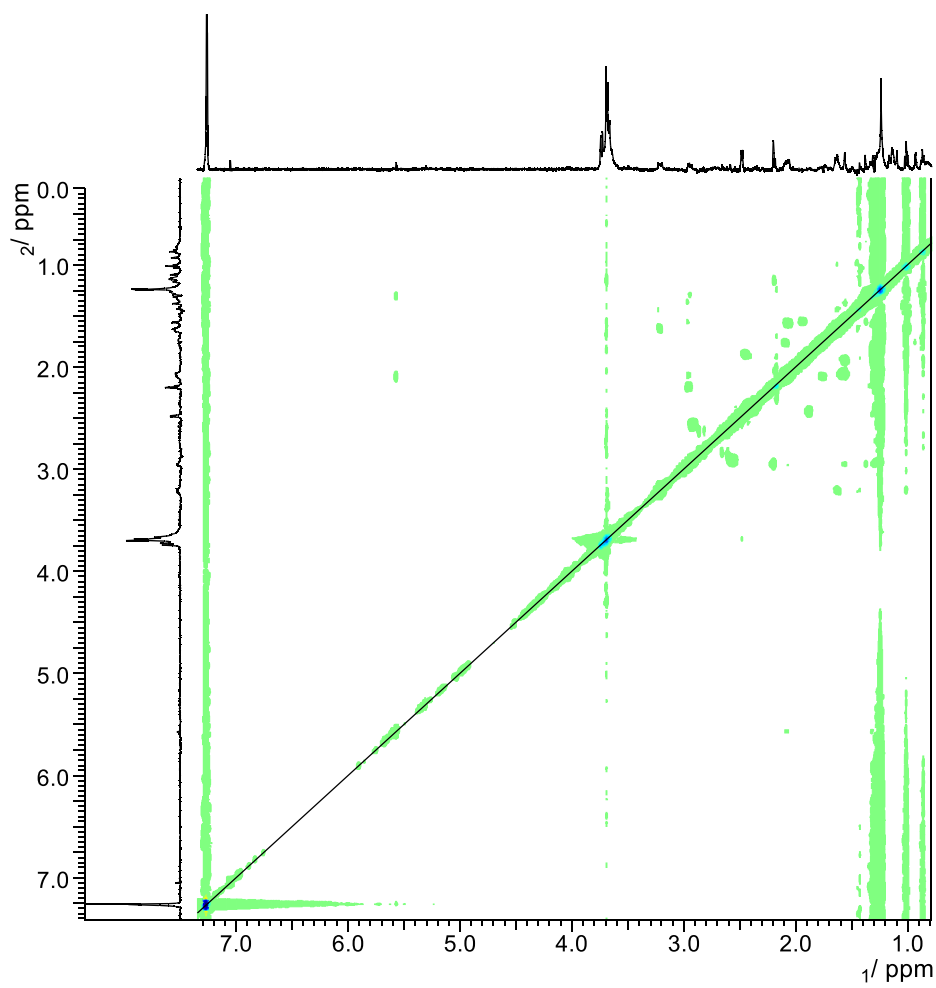


Figure S10. ^1H - ^1H -ROESY spectrum of **Ni-1**⁺ (500 MHz, CDCl_3 , 278 K, 4096 x 2048 p, 88 scans).

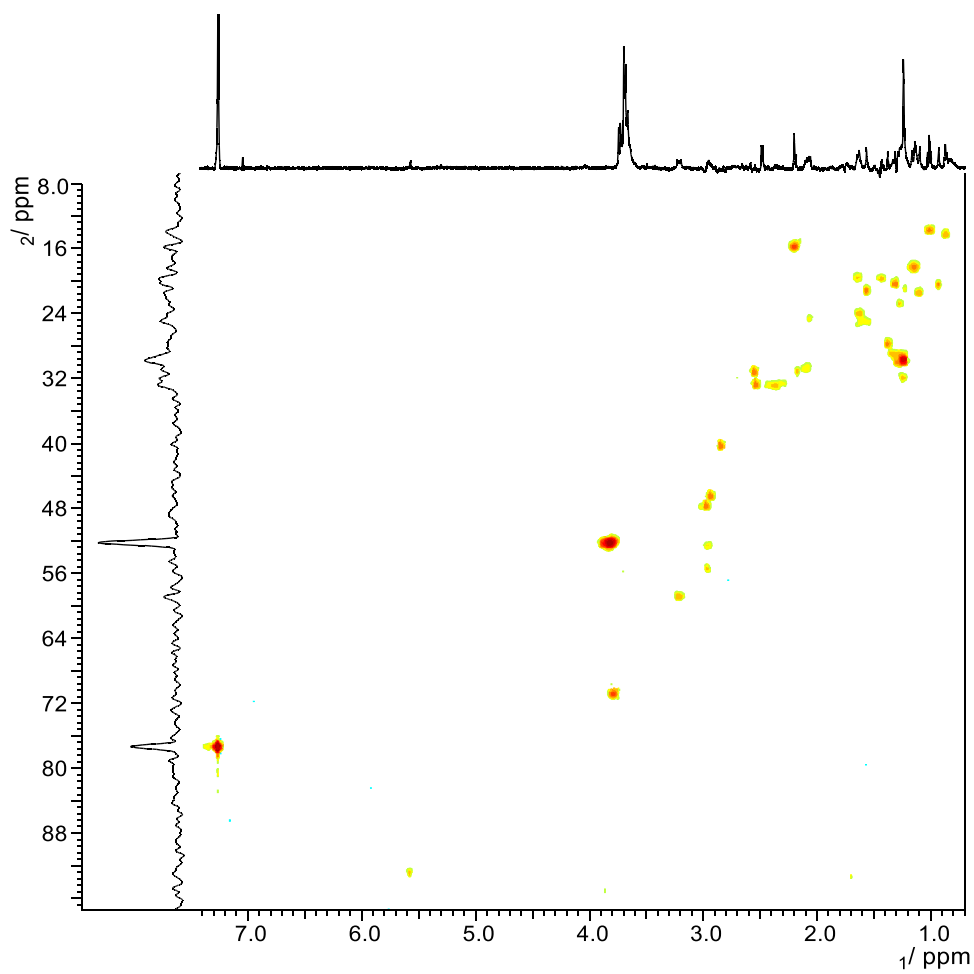


Figure S11. ^1H - ^{13}C -HSQC spectrum of Ni-1 $^+$ (500 MHz, 126 MHz, CDCl_3 , 278 K, 2048 x 4069 p, 180 scans).

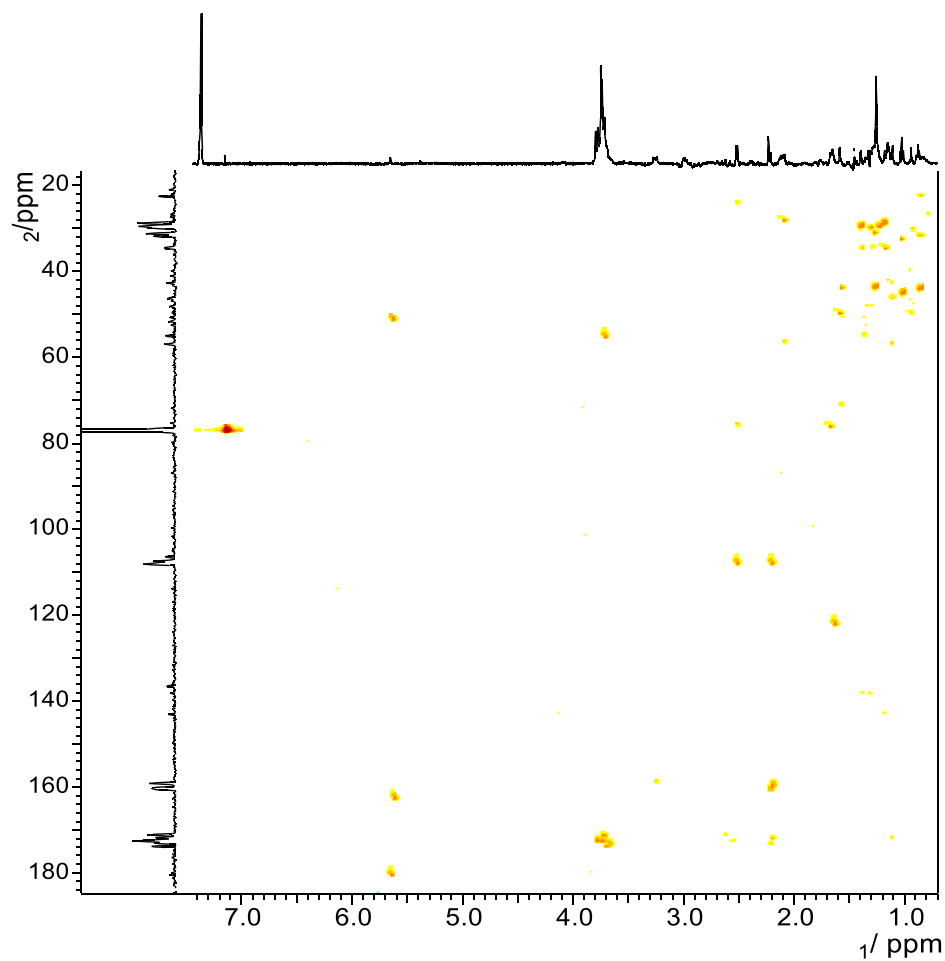


Figure S12. ^1H - ^{13}C -HMBC spectrum of Ni-1^+ (500 MHz, 126 MHz, CDCl_3 , 278 K, 1024 x 2048 p, 128 scans).

Table S1. ^1H -NMR chemical shifts and ^{13}C -NMR chemical shifts of Ni-1^+ .

Atom	$\delta(^{13}\text{C}) / \text{ppm}$	$\delta(^1\text{H}) / \text{ppm}$	Atom	$\delta(^{13}\text{C}) / \text{ppm}$	$\delta(^1\text{H}) / \text{ppm}$
C1	49.9	–	C2A	13.8	1.02
C10	92.8	5.57	C3	58.5	3.22
C11	181	–	C31	24.7	2.07/1.63
C12	49.5	–	C32	27.9	1.38
C12A	29.8	1.24	C33	172.6	–
C12B	20.5	0.94	C4	158.6	–
C13	30.7	2.92	C5	76.0	–

C131	31.2	1.74 / 2.56	C51	23.8	1.63
C132	34.3	1.26	C6	121.4	–
C133	172.6	–	C7	47.9	–
C14	159.8	–	C71	30.7	2.09/1.34
C15	107.5	–	C72	172.3	–
C151	15.2	2.2	C7A	20.5	1.32
C16	171.9	–	C8	55.2	3.22
C17	34.5	–	C81	19.6	1.63/1.44
C171	28.9	1.34 / 1.28	C82	30.1	1.01
C172	34.7	1.40 / 1.17	C83	173.8	–
C173	172.3	–	C9	<i>n.a.</i>	–
C17B	18.0	1.12	O5	–	2.46
C18	55.2	2.83	O6	–	2.47
C181	40.2	2.64	OC136	52.3	3.68
C182	171		OC176	52.3	3.73
C19	70.6	3.66	OC185	52.3	3.68
C1A	21.8	1.56	OC25	52.3	3.66
C2	44.9		OC36	52.3	3.7
C21	30.8	2.53/2.19	OC75	52.3	3.74
C22	173		OC86	52.3	3.68

EPR spectra.

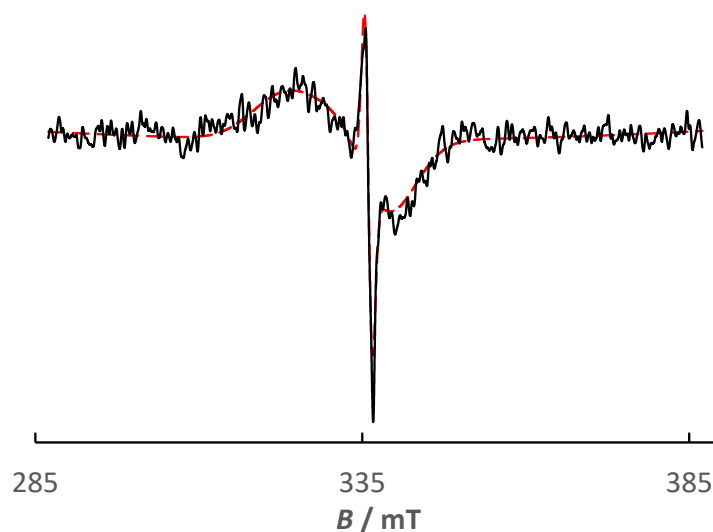


Figure S13. EPR spectrum of Ni-1^+ in frozen MeCN at 110 K. Conditions: $c \approx 2$ mM, microwave frequency 9.436 GHz. Broad signal: $g_{\parallel} = 2.194$, $g_{\perp} = 1.980$, obtained from simulation with *Easyspin* [easyspin.org], represented by the fitted red curve.

Note: In addition to the broad signal, a relatively sharp spike (1.3 mT p-p) with a symmetric feature centered around $g \approx 2$ is visible in S13. We assign the sharp signal with $g \approx 2.012$ to an impurity; most likely an organic radical generated during bulk electrolysis. Integration confirms that the spin count for the sharp signal is at least 26 times smaller than for the broad signal, which relates to 4 % (Figure S14). In the simulation it contributes 0.6%.

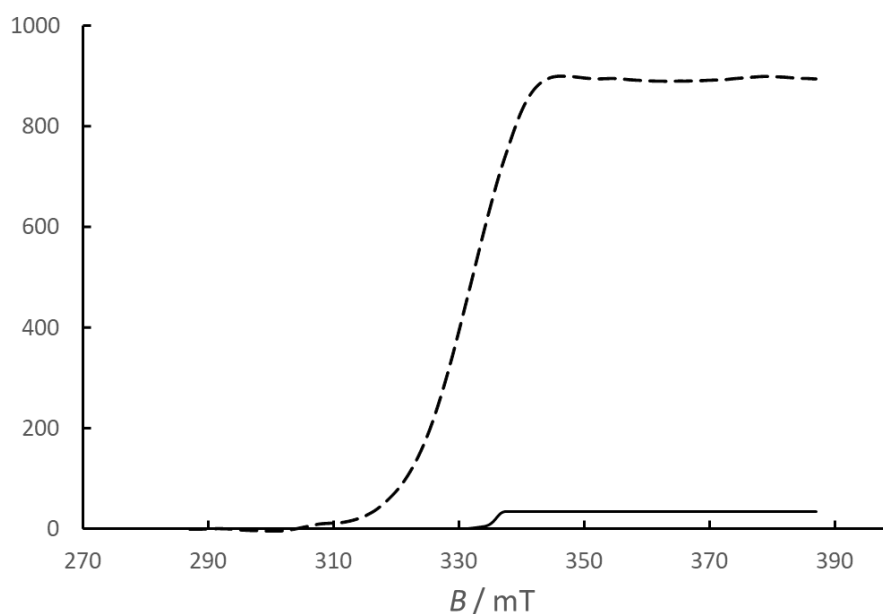


Figure S14. Double integration of the deconvoluted broad signal of Ni-1^+ (dashed line) in comparison with the superimposed sharp signal (solid line).

Electrochemical and Spectroelectrochemical data.

Cyclic Voltammetry:

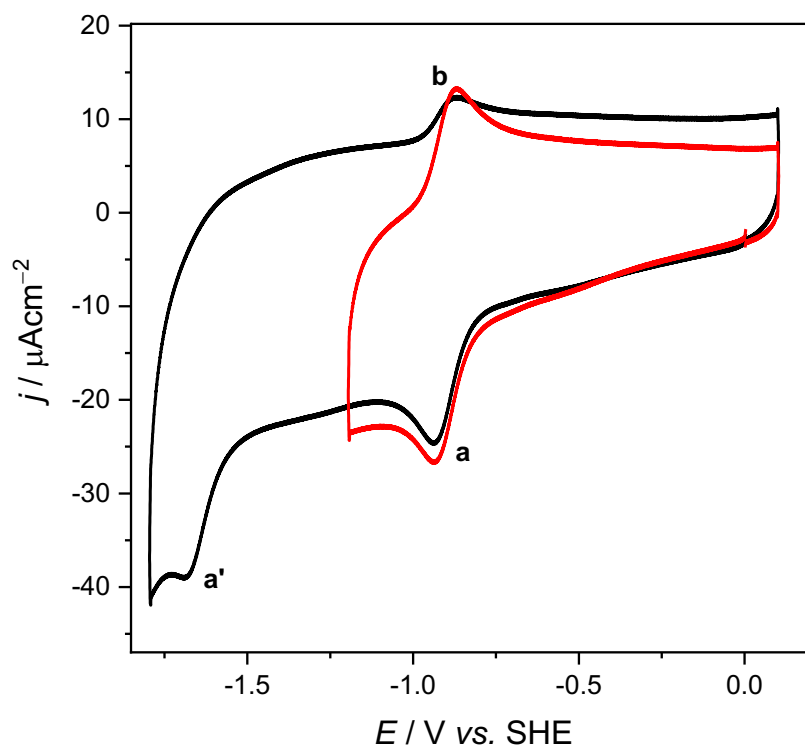


Figure S15. Cyclic voltammograms of **Ni-1**⁺ (0.68 mM) in DMF ([TBAPF₆] = 0.1 M). Scan rate 0.1 Vs⁻¹. Scans start at 0.0 V and revert at -1.2 V (red trace) or -1.6 V (black trace), revert again at 1.1 V and go back to 0.0 V.

Comment: Signals in the anodic return scan strongly depend on the potential of scan reversal (Fig. S15). When this lies beyond -1.2 V, the anodic wave *b* is decreased with respect to the cathodic wave *a*, pointing at reductive decomposition of **Ni-1**. A second, irreversible reduction wave *a'* appears at -1.7 V (Fig. S15), when the lower return potential is sufficiently negative.

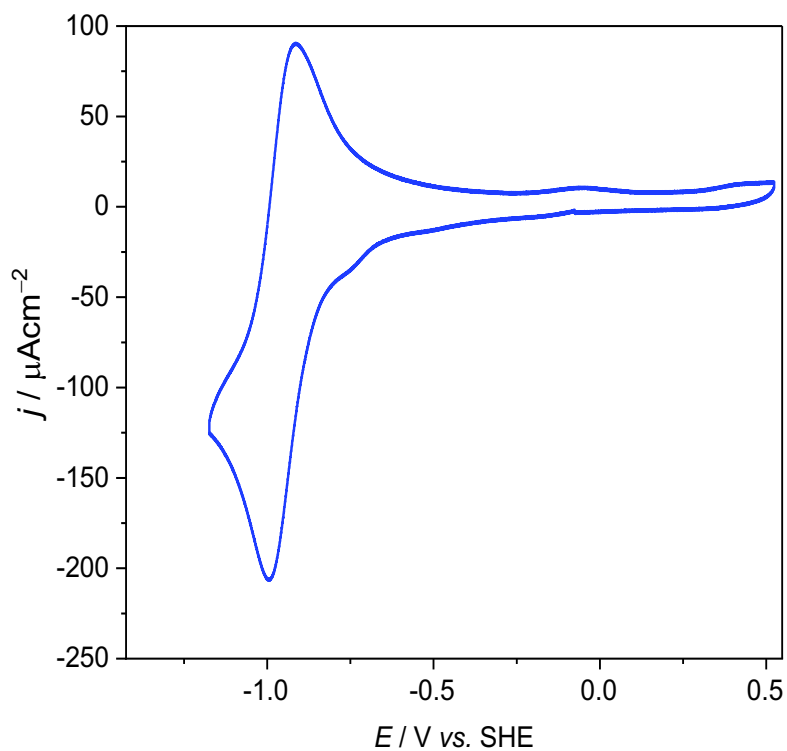


Figure S16. Cyclic voltammogram of Ni-1^+ (3.80 mM) in CH_3CN ($[\text{TBAPF}_6] = 0.1 \text{ M}$). Scan rate 0.1 Vs^{-1} . Scan starts at 0.0 V and reverts at -1.2 V , reverts again at 0.5 V and goes back to 0.0 V.

Spectro-electrochemistry:

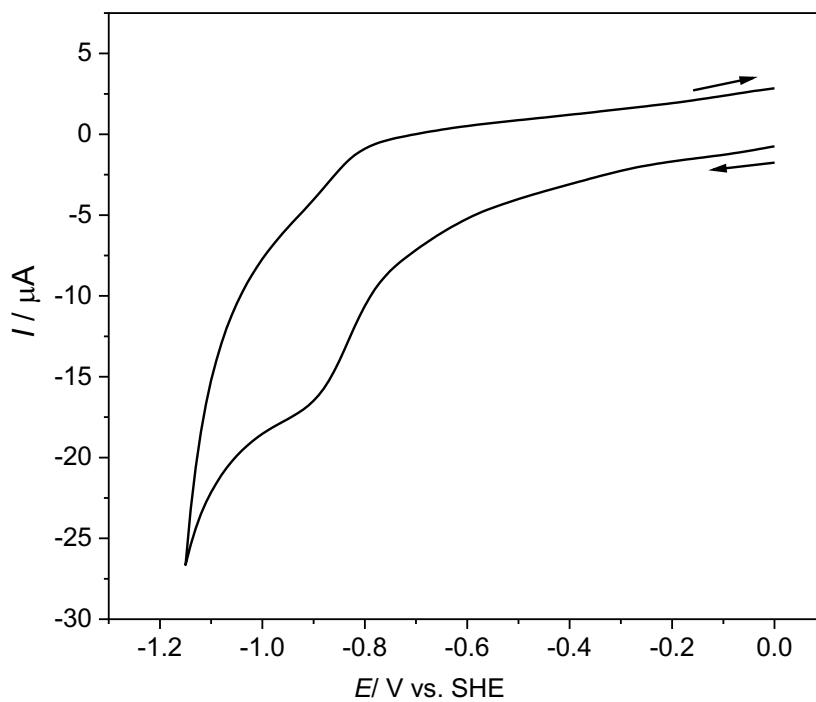


Figure S17. Cyclic voltammogram of Ni-1^+ (2.56 mM) in CH_3CN ($[\text{TBAPF}_6] = 0.6 \text{ M}$) recorded in the SEC cell. Arrows indicate direction of scan.

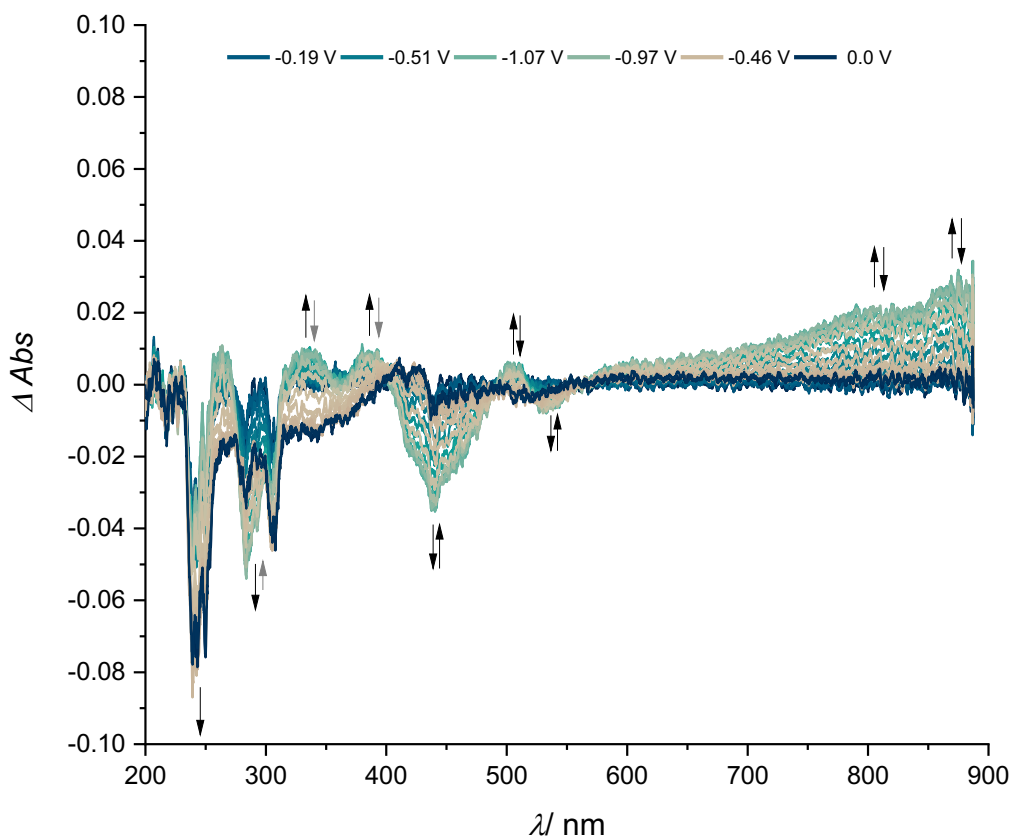


Figure S18. UV/Vis spectroscopic changes upon reduction of Ni-1^+ (2.56 mM) in a spectro-electrochemical cell in MeCN at the applied potential (see color chart). Arrows indicate the direction of spectral changes (grey arrows: no reversibility).

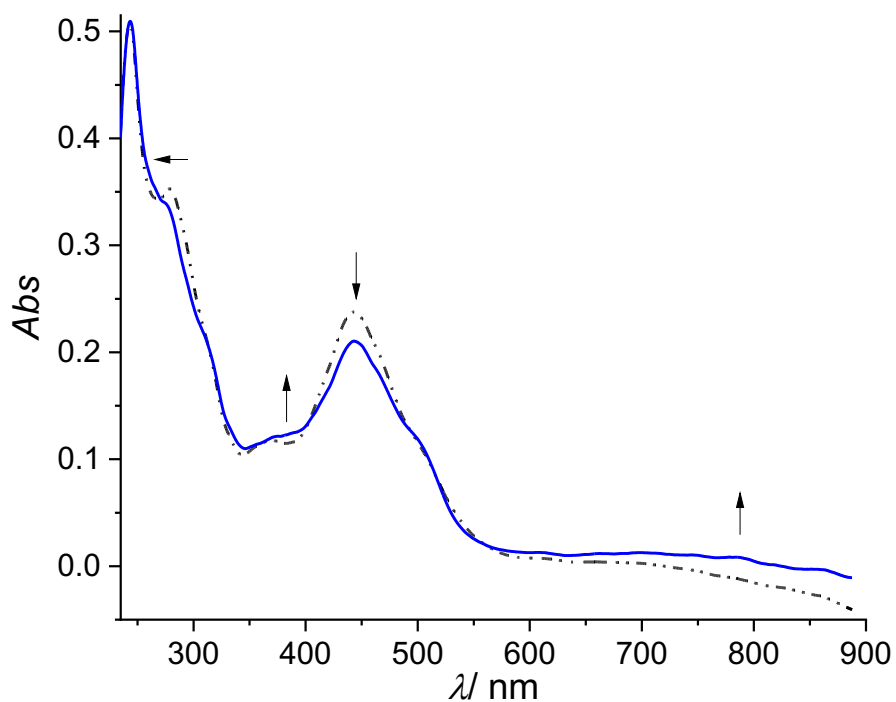


Figure S19. Absorption spectra (background corrected) of Ni-1^+ (at 0.0 V, black dashed-dotted line) and reduced Ni-1 (at -1.15 V, blue solid line) recorded in the SEC cell during cyclic voltammetry. Arrows indicate spectral changes.

Computational.

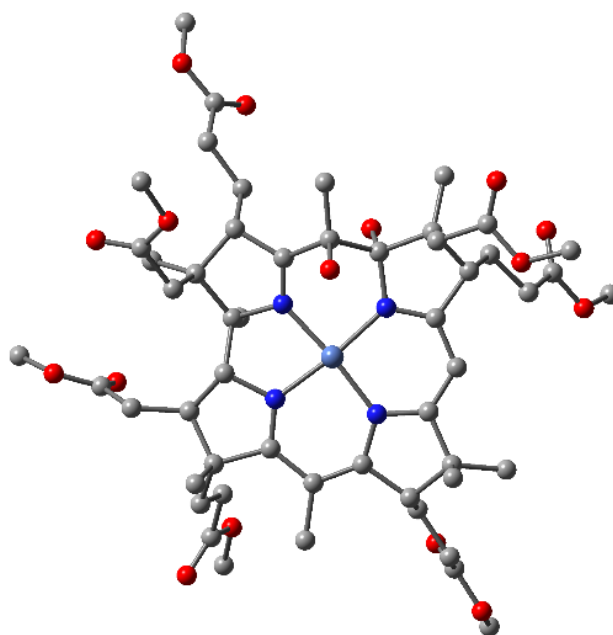


Figure S20. DFT optimized ground-state structure of Ni-1⁺.

Table S2. Coordinates of the DFT optimized ground-state structure of Ni-1⁺.

C	1.98639800	-1.43559800	0.03498000
C	3.57743200	-1.38996200	-0.11503600
C	3.87571600	0.13811200	0.13453700
C	2.58009400	0.77236500	-0.32422000
C	2.39742000	2.20635500	-0.85654400
C	1.14765900	2.81980600	-0.13907600
C	0.79748600	4.35098500	-0.39169800
C	-0.72820400	4.33591300	-0.04629000
C	-1.11125700	2.93990800	-0.48358900
C	-2.42203800	2.62608900	-0.88433800
C	-2.84752800	1.37632000	-1.26390200
C	-4.22134500	1.10175200	-1.86063100
C	-4.34860500	-0.42213400	-1.58237700
C	-2.88521200	-0.85221700	-1.50724800
C	-2.47093400	-2.16517100	-1.64112200
C	-1.10660800	-2.53031100	-1.38404700
C	-0.51583500	-3.95466200	-1.47480500

C	0.82276600	-3.76291500	-0.68306700
C	1.16691600	-2.29031800	-0.97560100
N	1.59128400	-0.04138600	-0.34072700
N	-0.09094500	2.09520800	-0.50105400
N	-2.09193800	0.23844800	-1.21031800
N	-0.17401000	-1.65245100	-1.08070300
C	1.50798600	-1.69370000	1.47602400
C	4.30970800	-2.34593200	0.83728600
C	4.25881300	0.58527400	1.57930000
C	5.77502800	0.61852600	1.80229000
C	6.15291800	1.05997300	3.20218300
O	5.37123700	1.41589800	4.06835900
O	7.48507700	1.01745600	3.38123700
C	7.98332700	1.42792900	4.67462600
C	3.66708100	3.04359500	-0.66102300
O	2.09569000	2.07571400	-2.25238900
O	1.40718400	2.66645100	1.26635200
C	1.61422500	5.33014700	0.46745100
C	0.93262700	4.71456200	-1.91168900
C	-1.09112100	4.63983300	1.43255700
C	-2.59889400	4.71265200	1.69346300
C	-2.92924700	5.16763100	3.10096000
O	-2.12239400	5.52760400	3.94219800
O	-4.25681800	5.13295800	3.32266600
C	-4.71167300	5.55844500	4.62653600
C	-5.34010000	1.99791400	-1.31108100
C	-4.11793800	1.32559900	-3.39468700
C	-5.06465100	-0.83319900	-0.26430400
C	-3.48761300	-3.21962500	-2.04873500
C	-0.26460100	-4.26631300	-2.97462900
C	-1.33996800	-5.10856800	-0.84637000
C	-1.85550200	-4.87190000	0.57864200

C	-2.74261700	-5.99692500	1.07471700
O	-3.02993700	-7.00534600	0.45142600
O	-3.18648400	-5.74893300	2.32054500
C	-4.04097800	-6.74862400	2.91984200
C	1.88943200	-4.83593400	-0.96697600
C	2.51994700	-5.43872400	0.27739700
O	2.06692600	-5.36524500	1.40745400
O	3.63465400	-6.11949500	-0.03125400
C	4.29016100	-6.82782600	1.04732100
H	-4.85817100	-0.90384300	-2.42108000
H	0.57120400	-3.83068000	0.37738800
H	1.63030300	-2.20233400	-1.96329500
H	1.78406400	-2.69490300	1.81482100
H	0.41864500	-1.60402800	1.52763300
H	5.39231200	-2.26547900	0.71632700
H	4.07244700	-2.16114900	1.88612700
H	4.04890300	-3.38435900	0.61809800
H	3.79273800	-0.06680200	2.32046100
H	3.85239400	1.58037000	1.77491800
H	6.25638900	1.30931000	1.09757400
H	6.23761800	-0.35837800	1.62389000
H	9.06561600	1.31971800	4.61271700
H	7.71141100	2.46785300	4.87070200
H	7.57644300	0.78317300	5.45715400
H	3.58700900	3.99245300	-1.19038400
H	3.86040700	3.25372600	0.39216800
H	4.53544400	2.52066500	-1.07255400
H	2.92460000	1.99803100	-2.75455000
H	0.90945500	1.89418600	1.58259300
H	1.14846200	6.32061500	0.45042500
H	1.66982600	4.99952300	1.50535600
H	2.63144900	5.45276900	0.08987700
H	0.30324900	4.05345000	-2.51145500
H	1.96005100	4.57609700	-2.24308100

H	-0.65393800	5.60911800	1.68876600
H	-0.63438000	3.90308700	2.09834600
H	-3.08930600	3.74565800	1.53633000
H	-3.08621400	5.41376600	1.00172000
H	-3.88940800	2.37291900	-3.61910600
H	-3.33708900	0.70028000	-3.84164600
H	-5.07318600	1.07119100	-3.86866200
H	-3.07241400	-3.92689600	-2.76833100
H	-4.35152000	-2.76940900	-2.53728900
H	-3.87086500	-3.80088900	-1.20157400
H	-1.19347100	-4.21674600	-3.54861100
H	0.13787700	-5.27651700	-3.10157900
H	0.43977300	-3.56004800	-3.42627000
H	-0.69389400	-5.99554500	-0.84067500
H	-2.17628500	-5.37462800	-1.49400000
H	-2.42667300	-3.93878100	0.65892900
H	-1.03444700	-4.77617300	1.29859600
H	-4.28122900	-6.36421300	3.91056500
H	-4.94939100	-6.87410000	2.32580700
H	-3.51153300	-7.70141900	2.99515700
H	2.67977300	-4.49797400	-1.64195300
H	1.43996300	-5.69396100	-1.48312700
H	5.15314700	-7.30945200	0.58931300
H	4.60681500	-6.12562400	1.82169900
H	3.61300500	-7.57221300	1.47238800
H	-4.67393800	-1.80285900	0.05889700
H	-4.80767700	-0.12844700	0.53435400
H	-5.79588300	5.45379200	4.60088100
H	-4.28234800	4.92065600	5.40285700
H	-4.43038200	6.59937100	4.80359300
H	-3.12641100	3.44542000	-0.94165500
H	-6.29533600	1.73913000	-1.77937800
H	-5.44992700	1.92208600	-0.22514000
H	-5.14624400	3.04774700	-1.55481600

C	0.58499200	6.15467500	-2.24391400
O	1.37247300	7.08642600	-2.20367600
O	-0.69921600	6.29842200	-2.62289000
C	-1.13027400	7.63232800	-2.97817700
H	-2.18087200	7.53191800	-3.24832500
H	-1.01378200	8.30650100	-2.12649800
H	-0.54814200	8.00061200	-3.82616500
H	-1.26067600	5.06761500	-0.66187700
H	1.93122900	-0.96734000	2.17236900
C	3.99427000	-1.71315700	-1.59128000
H	3.45189400	-1.06911200	-2.28887900
H	3.74518000	-2.75047200	-1.82045200
C	5.47908300	-1.58174800	-1.88732900
O	6.31125800	-2.44592300	-1.66808800
O	5.77871500	-0.39651500	-2.44927500
C	7.16628400	-0.16966700	-2.79316000
H	7.19272900	0.82603500	-3.23391500
H	7.78801700	-0.21218400	-1.89615100
H	7.49903600	-0.92002300	-3.51383700
H	4.68451200	0.46372000	-0.52479000
Ni	-0.23058300	0.20201300	-0.81489900
C	-6.58654200	-0.95859900	-0.39589600
H	-7.05908400	-0.01398900	-0.68362500
H	-6.84834000	-1.67475000	-1.18592900
C	-7.25257000	-1.42498000	0.88328400
O	-6.68443600	-1.66130900	1.93669200
O	-8.58277000	-1.55096700	0.72006100
C	-9.34242800	-1.98929800	1.86861600
H	-10.37719700	-2.03004700	1.53000400
H	-9.00416500	-2.97715300	2.19043700
H	-9.23415600	-1.27440800	2.68784100

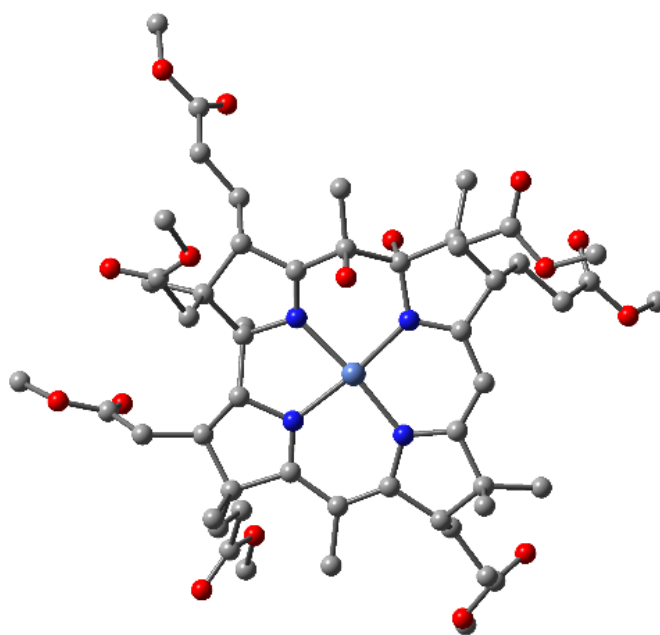


Figure S21. DFT optimized ground-state structure of Ni-1.

Table S3. Coordinates of the DFT optimized ground-state structure of Ni-1.

C	2.12471600	-1.32319200	0.01514000
C	3.69971300	-1.16930700	-0.23696400
C	3.94019500	0.34104700	0.16474400
C	2.56993300	0.93815000	-0.13138300
C	2.28885800	2.41864400	-0.51403000
C	0.90787400	2.92462900	0.07690100
C	0.49903300	4.45799800	-0.10240700
C	-1.06099900	4.34646600	0.04872100
C	-1.31598100	2.94792200	-0.49044100
C	-2.58799700	2.53734100	-0.97000400
C	-2.97469000	1.25268600	-1.33138800
C	-4.33094500	0.89810000	-1.95068900
C	-4.37995700	-0.64058600	-1.67195300
C	-2.88879100	-0.98718800	-1.53207400
C	-2.36751700	-2.28016900	-1.62016900
C	-0.97310900	-2.59165700	-1.36363300

C	-0.30451900	-3.98865300	-1.47048600
C	1.04348000	-3.71543900	-0.70585300
C	1.28528600	-2.21497300	-0.98706700
N	1.63577800	0.06594600	-0.19819300
N	-0.23701300	2.17936900	-0.45786600
N	-2.18526900	0.15270200	-1.23467500
N	-0.08430200	-1.66623800	-1.07026400
C	1.77474700	-1.71154300	1.46581900
C	4.56007400	-2.17899500	0.53620300
C	4.41283900	0.64100900	1.61888500
C	5.93717600	0.74929000	1.73861400
C	6.40298100	1.07339500	3.14371900
O	5.67848300	1.28666200	4.10183000
O	7.74675700	1.10477300	3.21530100
C	8.32420500	1.41546600	4.50305200
C	3.44852700	3.32673000	-0.07900700
O	2.19099100	2.41984200	-1.95389400
O	1.00182100	2.68575600	1.49704500
C	1.14793400	5.41463200	0.91209700
C	0.79086700	4.93618900	-1.56697700
C	-1.60428200	4.55141900	1.48806700
C	-3.13314100	4.58779500	1.57046500
C	-3.64570700	4.94256500	2.95102600
O	-2.95981400	5.16461900	3.93567900
O	-4.99302000	4.98371000	2.97351000
C	-5.61390000	5.30782800	4.23660000
C	-5.50651600	1.73283600	-1.42154800
C	-4.22807000	1.11947900	-3.48350400
C	-5.13052300	-1.08836300	-0.38729500
C	-3.32065700	-3.40379600	-2.00685000
C	-0.06254700	-4.29627500	-2.97167300
C	-1.04089200	-5.19130300	-0.82535500
C	-1.55818000	-4.97102800	0.60127300
C	-2.33623400	-6.15444900	1.13873900

O	-2.47981900	-7.22949500	0.57960700
O	-2.86129500	-5.88121900	2.34902600
C	-3.61285800	-6.93706600	2.98703800
C	2.17842000	-4.70641900	-1.02639000
C	2.82494900	-5.34591500	0.19013700
O	2.35875800	-5.36883800	1.31698000
O	3.98392800	-5.94332500	-0.13945000
C	4.67032500	-6.66262800	0.91058300
H	-4.83522900	-1.14781200	-2.52869400
H	0.81883900	-3.81525600	0.35800300
H	1.72387100	-2.10333300	-1.98462800
H	2.15191200	-2.70431000	1.72206200
H	0.68671000	-1.71577300	1.58668700
H	5.62318700	-2.02707400	0.33359600
H	4.40886100	-2.12006400	1.61572600
H	4.32928400	-3.20188000	0.22574700
H	4.04668700	-0.11887100	2.31192300
H	3.97010000	1.58075200	1.95892600
H	6.32412500	1.53462100	1.07540900
H	6.43765100	-0.17436300	1.42697400
H	9.40235600	1.39059800	4.34798600
H	8.00580500	2.40831500	4.82988200
H	8.02470000	0.66761600	5.24115100
H	3.37610400	4.30139000	-0.56192300
H	3.45835300	3.47805300	1.00195400
H	4.41005800	2.89612500	-0.37426700
H	3.08758000	2.42004700	-2.32992300
H	0.71935700	1.76430100	1.63494900
H	0.63335600	6.38114200	0.90623700
H	1.09985100	5.01104400	1.92462800
H	2.19468700	5.61379000	0.67255100
H	0.28924700	4.27398500	-2.27508100
H	1.85908000	4.88679400	-1.77337000
H	-1.22528800	5.50602200	1.86575700

H	-1.21424700	3.77357600	2.15013200
H	-3.57669200	3.62385100	1.29610400
H	-3.55102000	5.31990900	0.86589400
H	-4.05658200	2.17752900	-3.71189600
H	-3.40537500	0.53870900	-3.91628500
H	-5.15972500	0.80907800	-3.97304900
H	-2.87803400	-4.08817100	-2.73431200
H	-4.22625600	-3.01596200	-2.47466400
H	-3.64836500	-4.01162800	-1.15306700
H	-1.00260800	-4.28931300	-3.53029200
H	0.38425700	-5.28730200	-3.11158700
H	0.60032100	-3.55680500	-3.43444100
H	-0.34164200	-6.03773900	-0.81740500
H	-1.86802400	-5.51318900	-1.46145600
H	-2.20223900	-4.08621100	0.66872800
H	-0.73724900	-4.79068400	1.30613000
H	-3.95064400	-6.51765200	3.93428200
H	-4.46632300	-7.22168500	2.36701900
H	-2.97282500	-7.80603000	3.15863200
H	2.96347400	-4.27482200	-1.65426300
H	1.80065700	-5.55637000	-1.60928200
H	5.56538400	-7.06923200	0.44108600
H	4.93732900	-5.98151000	1.72182600
H	4.03634700	-7.46638000	1.29230100
H	-4.70450900	-2.03941800	-0.04998800
H	-4.95163000	-0.36851600	0.42005300
H	-6.68625100	5.28547100	4.04446100
H	-5.34371900	4.56618300	4.99223900
H	-5.30395100	6.30251500	4.56636700
H	-3.33158600	3.32058200	-1.06591500
H	-6.44070700	1.44167200	-1.91449300
H	-5.64023000	1.64082400	-0.33916000
H	-5.34982100	2.79374700	-1.64598500
C	0.38029000	6.36656400	-1.85885000

O	1.05895500	7.35271800	-1.61597400
O	-0.82514700	6.44432700	-2.45798900
C	-1.30274600	7.76619900	-2.79319000
H	-2.27436700	7.61086600	-3.26117500
H	-1.40314800	8.37266400	-1.88987200
H	-0.61355400	8.24984300	-3.48962300
H	-1.55220900	5.09090300	-0.58777600
H	2.18128600	-0.99299900	2.18078400
C	4.00519900	-1.30023400	-1.77043400
H	3.32815400	-0.66164800	-2.34367700
H	3.84603400	-2.33426000	-2.08634700
C	5.42753300	-0.96438600	-2.17841200
O	6.39106700	-1.70044500	-2.03859600
O	5.51439100	0.25430700	-2.74695400
C	6.82461900	0.67499800	-3.19165800
H	6.67796800	1.66698500	-3.61731500
H	7.51492300	0.71624700	-2.34597600
H	7.20349900	-0.01659700	-3.94775600
H	4.68482800	0.78040200	-0.50568100
Ni	-0.27004300	0.23956400	-0.76386300
C	-6.65020000	-1.29506900	-0.58447200
H	-6.82242800	-2.05093900	-1.35681400
H	-7.13330700	-0.36660500	-0.89666000
C	-7.30162100	-1.73073100	0.70890500
O	-7.57463500	-0.98209000	1.63529500
O	-7.52469200	-3.05763900	0.74879300
C	-8.10433200	-3.58474900	1.96325400
H	-8.19512800	-4.65759200	1.79658500
H	-7.44910900	-3.38124100	2.81356800
H	-9.08638500	-3.13805900	2.13626500

References.

- S1 I. Noviadri, K. N. Brown, D. S. Fleming, P. T. Gulyas, P. A. Lay, A. F. Masters and L. Phillips, *J. Phys. Chem. B*, 1999, **103**, 6713-6722.
- S2 M. Krejčík, M. Daněk and F. Hartl, *J. Electroanal. Chem. Interfacial Electrochem.*, 1991, **317**, 179-187.
- S3 Gaussian 09, Revision D.01, M. J. Frisch, G. W. Trucks, H. B. Schlegel, G. E. Scuseria, M. A. Robb, J. R. Cheeseman, G. Scalmani, V. Barone, B. Mennucci, G. A. Petersson, H. Nakatsuji, M. Caricato, X. Li, H. P. Hratchian, A. F. Izmaylov, J. Bloino, G. Zheng, J. L. Sonnenberg, M. Hada, M. Ehara, K. Toyota, R. Fukuda, J. Hasegawa, M. Ishida, T. Nakajima, Y. Honda, O. Kitao, H. Nakai, T. Vreven, J. A. Montgomery, Jr., J. E. Peralta, F. Ogliaro, M. Bearpark, J. J. Heyd, E. Brothers, K. N. Kudin, V. N. Staroverov, T. Keith, R. Kobayashi, J. Normand, K. Raghavachari, A. Rendell, J. C. Burant, S. S. Iyengar, J. Tomasi, M. Cossi, N. Rega, J. M. Millam, M. Klene, J. E. Knox, J. B. Cross, V. Bakken, C. Adamo, J. Jaramillo, R. Gomperts, R. E. Stratmann, O. Yazyev, A. J. Austin, R. Cammi, C. Pomelli, J. W. Ochterski, R. L. Martin, K. Morokuma, V. G. Zakrzewski, G. A. Voth, P. Salvador, J. J. Dannenberg, S. Dapprich, A. D. Daniels, O. Farkas, J. B. Foresman, J. V. Ortiz, J. Cioslowski, and D. J. Fox, Gaussian, Inc., Wallingford CT, 2013.
- S4 A. D. Becke, *J. Chem. Phys.*, 1993, **98**, 5648-5652.
- S5 R. Ditchfield, W. J. Hehre and J. A. Pople, *J. Chem. Phys.*, 1971, **54**, 724-728.
- S6 M. Cossi, N. Rega, G. Scalmani and V. Barone, *J. Comput. Chem.*, 2003, **24**, 669-681.
- S7 R. Bauernschmitt and R. Ahlrichs, *Chem. Phys. Lett.*, 1996, **256**, 454-464.
- S8 S. M. Chemaly, M. Florczak, H. Dirr and H. M. Marques, *Inorg. Chem.*, 2011, **50**, 8719-8727.
- S9 L. Werthemann, Dissertation ETH Zürich, Juris Verlag, Zürich, 1968.
- S10 B. Kräutler and R. Stepánek, *Helv. Chim. Acta*, 1985, **68**, 1079-1088.
- S11 C. Brenig, L. Prieto, R. Oetterli and F. Zelder, *Angew. Chem. Int. Ed.*, 2018, **57**, 16308-16312.